Reconstructing mass balance of South Cascade Glacier using tree-ring records

Kailey Marcinkowski

A thesis

submitted in partial fulfillment of the

requirements for a degree of

Master of Science

University of Washington

2012

Committee:

Gregory J. Ettl

David L. Peterson

Don McKenzie

Andrew Fountain

Program Authorized to Offer Degree:

School of Environmental and Forest Sciences

ABSTRACT

Mountain hemlock growth chronologies were used to reconstruct the mass balance of South Cascade Glacier, an alpine glacier in the North Cascade Range of Washington State (USA). The net balance reconstruction spans 350 years, from 1659 to 2009. Summer and winter balances were also reconstructed for 1346-2009 and 1615-2009, respectively. Relationships between mass balance and winter precipitation, temperature, the Pacific Decadal Oscillation index, and the El Niño Southern Oscillation index suggest that these climatic variables and indices influence glacier balance fluctuations at various temporal scales. Periods of above-average net, summer, and winter mass balance occurred mainly in 1790-1800, 1810-1820, 1845-1860, 1865-1890, and 1970-1990. Above- and below-average reconstructed mass balances at South Cascade Glacier were concurrent with similar periods from other glacier balance reconstructions and moraine dates in the Pacific Northwest region of North America. Agreement among these records suggests that changes in South Cascade Glacier mass balance are good indicators of regional balance fluctuations, and glaciers in the Pacific Northwest are responding similarly to regional external climate forcings. The current rate of decline, from 2000 to 2009, in the reconstructed mass balance record has been faster than any other decline in a century. This decreasing trend is projected to continue in accordance with increasing temperatures, and will likely affect glacier-influenced water resources in the Pacific Northwest.

TABLE OF CONTENTS

LIST OF FIGURES

Figures Page

LIST OF TABLES

ACKNOWLEDGEMENTS

I would like to thank the members of my committee, Greg Ettl, Don McKenzie, and Andrew Fountain for their guidance, support, and advice during the thesis process. I would especially like to thank David L. Peterson for giving me the opportunity to pursue this research. He has been a wonderful advisor, with his talent for teaching and enthusiasm for the subject matter, and it is because of his support, encouragement, and belief in my abilities that I have come so far these past two years.

Maureen Kennedy's statistical and programming assistance was invaluable to me as I was conducting this research. She was always available to patiently answer my questions, no matter how big or small, talk about concepts, and provide explanations I could understand. Whenever I created a new script in R, I would share my excitement with Maureen, who would be just as delighted. Her mastery of R programming was an inspiration to me, and I thoroughly enjoyed learning code from her.

Thank you to Rob Norheim for his excellent GIS skills and his willingness to volunteer for field work assistance. Thank you to my peers in the Fire and Mountain Ecology Lab, who were wonderful examples of scientists. I am especially grateful to Joe Restanio for introducing me to wilderness field work. His endless patience with my lack of wilderness skills helped me gain confidence in the backcountry.

I would like to thank Bill Bidlake and the USGS Water Science Center in Tacoma. Bill supported this project wholeheartedly, and his knowledge of South Cascade Glacier was invaluable to me. Without him, I would never have been able to experience South Cascade Glacier firsthand. The opportunity to helicopter in and stay at one of the most beautiful places on Earth was amazing, and I will never forget it.

The support for this research was funded by the U.S. Geological Survey Global Change Research Program through the Western Mountain Initiative. Funding was also provided by a fellowship from the School of Environmental and Forest Sciences at the University of Washington.

I am also thankful for the support of my family and friends. My friends were wonderful for comic relief and sharing ideas, and the support they have shown me is boundless. I would particularly like to thank my parents, who have always believed I can do anything. My mother has set an example that has shaped me into the person I am today, and my father's intelligence and work ethic have inspired me to reach higher. Lastly, I would like to thank my husband, Brian. His unwavering support of all my endeavors has meant the world to me. I would not have been able to do this without him.

DEDICATION

To my husband.

INTRODUCTION

Since the 1980s, the majority of alpine glaciers in the Pacific Northwest (PNW) region of North America have receded faster than the glacier recession documented in the early 20th century (Hodge et al. 1998; Meier et al. 2003; Granshaw and Fountain 2006; Pelto 2006; Koch et al. 2009; Moore et al. 2009). This rapid retreat is frequently attributed to a shift in atmosphere and ocean circulations in the mid-1970s resulting in increased temperatures (McCabe and Fountain 1995; McCabe et al. 2000; Moore and Demuth 2001; Rasmussen and Conway 2004). Alpine glaciers are sensitive to such variations in climate, and these changes are represented by fluctuations in the terminus and volume of the glaciers. Because of complex ice dynamics, the response of the terminus to climate is delayed. Changes in glacier volume are typically assessed using mass balance measurements, which reflect an immediate response to climate (Walters and Meier 1989).

Similar climatic variables influence both mass balance fluctuations and tree radial growth. Because of this mutual relationship with climate, tree-ring chronologies can be used as proxies for glacial mass balance (Lewis and Smith 2004; Watson and Luckman 2004; Larocque and Smith 2005; Wood et al. 2011). Mountain hemlock (*Tsuga mertensiana*) is often chosen as a proxy for glacial mass balance because it grows at high elevations and experiences similar climatic regimes as glaciers. South Cascade Glacier, in the Cascade Range in northern Washington State (USA), is a prime location to reconstruct glacial balance because of its relatively long time series of mass balance measurements. In this study, mountain hemlock growth chronologies were used to assess historical variability of South Cascade Glacier (SCG) mass balance.

Glacier net mass balance (b_n) is the sum of winter mass balance (b_w) and summer mass balance (b_s).

$$b_n = b_w + b_s$$

Winter balance (usually > 0) is composed of accumulations in the form of snow or ice; summer balance (usually < 0) reflects ablation such as melting, sublimation, or ice calving. Mass balance is measured in meters of water equivalent (m w.e). Although it is generally assumed that summer temperature and winter precipitation drive mass balance fluctuations, this assumption greatly simplifies the relationship between climate and mass balance, which is complicated by glacial ice dynamics (Burbank 1982; Bitz and Battisti 1999). In maritime climates, west of the Cascade Range in Washington State, winter precipitation, and therefore winter mass balance, dominates net mass balance (Bitz and Battisti 1999; Dyurgerov and Meier 1999). Glaciers that are further south or further inland tend to be more sensitive to summer temperature, in addition to winter precipitation (Walters and Meier 1989; Hodge et al. 1998; Dyurgerov and Meier 1999).

The weather patterns of the PNW affect glacier mass balance, on both a short-term scale and an inter-decadal scale. These weather patterns include atmospheric circulation anomalies (McCabe and Fountain 1995; McCabe et al. 2000; Meier et al. 2003; Rasmussen and Conway 2004; Shea and Marshall 2007), sea surface temperatures and pressures (Hodge et al. 1998; Bitz and Battisti 1999; Moore and Demuth 2001; Kovanen 2003; Pederson et al. 2004; Watson et al. 2006; Pelto 2008), and averaged climatic variables such as annual or seasonal surface air temperature and precipitation (Burbank 1982; Oerlemans et al. 1998; Rasmussen 2009; Sitts et al. 2010; Wood et al. 2011). Glacier mass balance also responds to storm tracks moving through the PNW (McCabe and Fountain 1995; Hodge et al. 1998; Bitz and Battisti 1999; McCabe et al. 2000).

One of the atmospheric systems influencing mass balance in the PNW is the Aleutian Low, a low-pressure cell that affects climate and storminess on a seasonal scale. During winter months, the Aleutian Low settles over the Aleutian Islands in the North Pacific, bringing strong onshore flow and storms over Washington State. The Aleutian Low weakens and moves north during the summer, being replaced by a sub-tropical high pressure cell, and as a result the Northwest experiences fairer weather and fewer storms (Phillips 1965).

The severity and magnitude of the Aleutian low is affected by the El Niño Southern Oscillation (ENSO), an interannual mode of climatic variability. Above-average sea surface temperatures in the western tropical Pacific Ocean are indicative of El Niño, and below-average sea surface temperatures characterize La Niña (Rasmussen and Wallace 1983). El Niño winters tend to have a deepened Aleutian low that shifts southeast of its normal position, causing warm dry air to flow into the Northwest. Conversely, La Niña winters generally cause a weakened Aleutian low, where the storm track is either shifted directly at the PNW or into Alaska and down through British Columbia, bringing more storms and cooler temperatures into Washington State than do El Niño winters. Differences in ENSO phases are correlated with increases and decreases in glacier mass balance (Hodge et al. 1998; Bitz and Battisti 1999; Moore and Demuth 2001; Larocque and Smith 2005; Watson et al. 2006; Pelto 2008; Wood et al. 2011).

The Pacific Decadal Oscillation (PDO), another mode of climatic variability, is distinguished by changes in sea surface temperature, sea level pressure, and wind patterns. PDO has cool and warm phases, each lasting 20-30 years (Mantua 1997). The cool phase of PDO is similar to La Niña events, with cool wet weather experienced in the PNW, and the warm phase is analogous to the drier warmer El Niño. Many studies have documented correlations between the annual and seasonal PDO index and fluctuations in glacier mass balance (Hodge et al. 1998; Bitz

and Battisti 1999; Moore and Demuth 2001; Kovanen 2003; Lewis and Smith 2004; Pederson et al. 2004; Larocque and Smith 2005; Watson et al. 2006; Pelto 2008; Wood et al. 2011).

Different weather systems affect not only glacier mass balance, but also other climate-sensitive natural resources in the PNW. High-elevation tree species respond to similar climatic variables and patterns as glacial mass balance. For example, mountain hemlock growth at high elevations (>1500 m) is particularly sensitive to winter precipitation, in the form of snowpack, which affects the length of growing season (Peterson and Peterson 2001). Mountain hemlock growth is also correlated with winter PDO index (Gedalof and Smith 2001a; Peterson and Peterson 2001). These responses to climate are observed in tree radial growth. Favorable growth periods of mountain hemlock are associated with less snowpack and a longer growing season, which produce wider rings, and unfavorable growth periods are characterized by deeper snowpack and a shorter growing season, which create narrower rings.

Glacier mass balance should therefore be inversely related to mountain hemlock radial growth. Favorable growth for mountain hemlock coincides with the conditions that influence negative mass balance, and below-average growth occurs during states attributed to positive mass balance. Therefore, it is reasonable to assume that tree-ring width chronologies can be used as a proxy for reconstructing glacier mass balance. Because mountain hemlock trees are long-lived, such chronologies could allow for a reconstruction of changes in mass balance back to many years before the observational record began.

In the PNW, Lewis and Smith (2004) used mountain hemlock chronologies to reconstruct the mass balance of two glaciers on Vancouver Island, British Columbia (Canada). Watson and Luckman (2004) reconstructed mass balance at Peyto Glacier, also in British Columbia, from regional precipitation and temperature reconstructions using various tree species as proxies.

Larocque and Smith (2005) examined correlations for the mass balance of several glaciers and the radial growth of several tree species to reconstruct a regional mass balance record for glaciers in the PNW, including SCG winter balance (since 1835). The SCG winter balance reconstruction used mountain hemlock growth chronologies from Oval Glacier near Mount Waddington, British Columbia, which is about 450 km northwest of SCG. Wood et al. (2011) reconstructed mass balance of Place Glacier in British Columbia from tree-ring width and maximum ring density chronologies of Engelmann spruce (*Picea engelmannii*).

Examining past SCG mass balance changes and future rates of decline has broader applications to other glaciers with similar climatic regimes and topographic features. Changes in year-to-year net balance at SCG are correlated with those of surrounding glaciers (Pelto 2008; Fountain et al. 2009), and similarly to trends at SCG, the majority of glaciers in the PNW have been receding (Hodge et al. 1998; Granshaw and Fountain 2006; Pelto 2006; Koch et al. 2009). Because of this connection, regional glacier mass balance can be expected to follow trends at SCG.

Ongoing reduction in regional mass balance will eventually affect water resources, because glacier meltwater supplements many streams in the PNW (Moore et al. 2009; Nolin et al. 2010). Glaciers influence streamflow by storing water as ice during periods of high precipitation and cool temperatures and releasing it as meltwater during drier or warmer times (Fountain and Tangborn 1985). Mountain snowpack has been decreasing in the PNW over the last 40 years (Mote et al. 2005; McCabe and Wolock, 2010; Pederson et al. 2011). Decreased snowpack reduces storage and meltwater available for streamflow. Reduction in late-summer flows has been observed and modeled for many glacier basins in the PNW (Granshaw and Fountain 2006; Stahl and Moore 2006; Moore et al. 2009; Nolin et al. 2010; Pelto 2011).

In this study, we expand on Larocque and Smith (2005) by (1) focusing solely on SCG, (2) sampling sites closer to SCG, and (3) using longer tree-ring chronologies (starting 1659 vs. 1835). Specifically, we reconstructed SCG net, summer, and winter mass balance. Mountain hemlock growth chronologies were obtained from four sites surrounding SCG in the North Cascade Range, Washington State. Closer proximity of sampling sites and a longer reconstruction interval are expected to produce a more robust analysis of past mass balance at SCG. The main objective of this study is to assess both past mass balance variability and current recession at SCG. The extent of the reconstruction is limited by the ages of the chronologies but extends the mass balance record by several hundred years into the past. Dated periods of above- or below-average mass balance at SCG are evident from the time series and are useful in identifying if mass balance changes in the last century are comparable to those of previous centuries. Other glacier mass balance reconstructions and moraine dates from the region are compared to the SCG reconstruction to evaluate whether a broad synchrony in past mass balance exists. Comparisons are also made with reconstructions of PDO and ENSO indices in order to determine if current relationships that appear to govern SCG mass balance are consistent with the past. Rates of change between periods of positive and negative reconstructed mass balance are calculated to provide a context for the recent decline. These mass balance rates are matched to projected increases in future temperature to estimate future mass balance decline.

METHODS

Study site

South Cascade Glacier (SCG) is located at 48° 21′ 19″ N, 121° 3′ 27″ W within the North Cascade Range in Washington State (USA). The glacier is in a north-northwest facing valley with an altitude range of 1600 to 2100 meters (Bidlake et al. 2010). Meltwater from the glacier flows into South Cascade Lake, the headwaters of the South Fork of the Cascade River. The South Fork connects with the Skagit River and empties into Puget Sound.

SCG is an ideal location for conducting reconstructions of mass balance because it has one of the longest, most complete records of mass balance measurements in North America. The U.S. Geological Survey (USGS) has taken annual measurements at SCG since 1959. SCG and two other valley glaciers in Alaska are used as benchmark glaciers by the USGS for the PNW. Benchmark glaciers are considered representative of glaciers within a region and are measured annually for mass balance, runoff, glacial geometry, and weather (Fountain et al. 2009). Annual fluctuations in net mass balance at SCG are highly correlated with those of surrounding glaciers and thus can be interpreted as representative of year-to-year mass balance variations (Pelto 2008; Fountain et al. 2009). Over the five decades of USGS monitoring, SCG has retreated 0.7 km from its 1958 terminus position, and the area has shrunk from 2.71 km^2 in 1958 to 1.73 km^2 in 2007 (Bidlake et al. 2010). Net, winter, and summer mass balance values for 1959-2009 were used in this study (Bidlake et al. 2010 [1959-2007]; W.R. Bidlake, *personal communication*, 2011 [2008-2009])

Because of its long record, mass balance at SCG has been the subject of many studies. Mass balance models based on meteorological variables, such as temperature and precipitation,

have been used to estimate SCG seasonal and net mass balance (Tangborn 1980, 1999; Rasmussen and Krimmel 1999; Rasmussen and Conway 2001, 2003; Rasmussen 2009). SCG mass balance has also been linked with atmospheric and ocean circulation indices (McCabe and Fountain 1995; Hodge et al. 1998; Bitz and Battisti 1999; McCabe et al. 2000; Larocque and Smith 2005).

Chronology construction

Four high-elevation forests dominated by mountain hemlock and surrounding SCG in the North Cascade Range were sampled in summer 2011 (Table 1). All sites were within a 75-km radius of SCG (Figure 1). Twenty trees were sampled at each site, with preference given to the largest, dominant, or co-dominant trees without obvious signs of disturbances (i.e. fire, insects, wind) or breakage. Trees were sampled at breast height with an increment borer at the cross-slope position of the bole in order to reduce the likelihood of encountering compression wood. Cores were stored in paper straws and handled carefully during transportation from field to lab.

The cores were air dried and glued to slotted mounting boards. Cores were sanded with progressively finer grades of sandpaper until the ring pattern was clearly visible and annual ring boundaries were easy to identify. The tree rings were crossdated using standard dendrochronology procedures (Stokes and Smiley 1968). For each tree, the core with the most intact or longest record was chosen, and the ring widths were measured and recorded to the nearest 0.001mm using *MeasureJ2x* (Version V4.2 [software]. 2010) and an Olympus DF PLAN 1.5x measuring scope. Crossdating was verified, and any missing or false rings were corrected, using the program COFECHA (Holmes 1983).

Tree-ring series were detrended with ARSTAN (Cook and Holmes 1996). Detrending is used to remove trends caused by tree age and growth characteristics. When trees first establish, rings are wide because the circumference of the tree is small, but as the tree ages the widths of the rings decrease to accommodate increasing circumference. There are many techniques that can be applied to remove these trends. Several curves were explored before a cubic spline with a 50% cutoff of 150 years was chosen (Table 2). Upon examination of curve statistics, such as mean sensitivity and interseries correlation, it was decided that splines of different smoothness had similar results. Mean sensitivity describes the average interannual change between ring widths, and interseries correlation is the average correlation between pairs of series and the master chronology and is considered a measure of the strength of a common signal in the chronologies (Fritts 1976).

The stiff cubic spline was selected because the majority of the trees sampled did not display typical juvenile growth in the innermost rings or a negative exponential decline afterward. Most trees were older than 250 years and usually were rotten towards the middle, so often the pith was not recovered. This led to most series exhibiting the radial growth trend of mature trees. For the few trees that did seem to have an age-related decline, the stiff spline matched the curve as well or better than a negative exponential fit. A double-detrending method using a negative exponential and cubic spline curves was considered for those trees, but was disregarded in favor of applying the same curve fit for all series.

A unitless index was then calculated for each detrended series by dividing the measured observations by the fitted curve values for easier comparisons and averaging between individual series. The indexed series were then prewhitened to remove autocorrelation effects from the biological persistence of individual trees. Examination of the autocorrelation and partial

autocorrelation functions showed that an autoregressive model (AR) would be best for prewhitening. AR modeling generates a residual chronology for the ring-width series that is uncorrelated with past or future values. The series were then averaged into site chronologies using a bi-weight robust mean. The calculation of indices, AR models, and site chronologies was done using ARSTAN (Cook and Holmes 1996).

Principal components analysis (PCA) was conducted on the four residual site chronologies to identify the common variance between the different sites. Because the sites were spread out around SCG, we wanted to find a commonality between them that might better represent changes in SCG mass balance and add strength to our results. A common interval of 1659-2009 was used. The ending point for this interval is the last year of mass balance measurements currently available, and the starting date is the earliest year of the shortest growth chronology among the four sites.

Climate data

Divisional climatic data were obtained from the National Climatic Data Center (http://www.ncdc.noaa.gov/oa/ncdc.html). Divisional data are a compilation of individual stations within regions thought to have similar climate, and were chosen for this analysis over individual station data for several reasons. Because the divisional data are derived from multiple stations, they better represent regional climate and have a longer record than any one station. The sites sampled had no local long-term weather stations. Monthly precipitation, temperature, and the Palmer Drought Severity Index (PDSI) were used from two climatic divisions; the Hidden Lake (HL), South Cascade (SC), and Bagley Lakes (BL) sites, and SCG all fell within the boundaries of the western Washington Cascades, and the Minotaur Lake (ML) site was

located in the eastern Washington Cascades. The Park Creek Ridge SNOTEL site was used for the April 1st snow water equivalent (SWE) record, and the Park Creek Ridge snow course record was used for April 1st snow depth. Park Creek Ridge was chosen because it is the closest observation site to SCG.

Several observed ocean indices were obtained from various sources. The Pacific North American index (PNA) was obtained from the National Weather Service Climate Prediction Center (http://www.cpc.ncep.noaa.gov/products/precip/CWlink/daily_ao_index/teleconnections.shtml); the Pacific Decadal Oscillation index (PDO) was found in the Joint Institute for the Study of the Atmosphere and Ocean climate data archives (http://jisao.washington.edu /pdo/PDO.latest); and the Niño Region 3.4 Index (ENSO) was retrieved from the National Center for Atmospheric Research (http://www.cgd.ucar.edu/cas/catalog/climind/TNI_N34 /index.html#Sec5). These indices were chosen to explore which ocean-atmospheric circulation modes affect tree growth and SCG mass balance.

The residual chronologies from all four sites were compared to the current water year (October-September) and previous water year divisional climatic data and ocean indices by month using Pearson product-moment correlations. Net, summer, and winter measured mass balance values were also compared to current and previous-year climatic and circulation variables using product-moment correlations. Correlations were calculated for April 1st SWE, April 1st snowpack depth, total winter (October-March) precipitation, and average winter and spring (March-May) PDO and ENSO indices with the four residual chronologies and the observed mass balance data.

Mass balance reconstruction

Pearson product-moment correlations were calculated between each of the four residual chronologies and the first principal component (PC1) derived from the PCA and summer, winter, and net mass balance measurements. This was done to determine if there was a statistically significant relationship between the site chronologies and the mass balance measurements. Simple linear regression analyses were conducted for each of the chronologies and PC1 with net, summer, and winter mass balance, where mass balance was the dependent variable and site-specific growth indices the independent variable. Multiple regression using growth from the current year plus growth from the previous year was also explored as a reconstruction option, but was not found to be meaningful. Coefficients of determination (R^2) were calculated for each regression model, and residuals were examined for departures from normality and autocorrelation. When a significant relationship ($p<0.05$) between tree growth and mass balance existed, the growth indices were used in the regression equation to reconstruct mass balance. R^2 was used as the criteria for choosing which regression model was used to represent net, winter, and summer balance in this study. All calculations and graphs in this study were created using R (Version 0.94.110 [software]. R Core Development Team 2010).

RESULTS

Climate-growth correlations

Correlations between monthly circulation indices and tree growth were explored at the four sampling sites (Fig. 2, 3). Of the circulation indices, PNA did not have significantly strong correlations or agreement among the sites. December, January, and April PDO were positively correlated to tree growth. In the year prior to growth, November and December PDO were negatively related at the four sites, with October and February also significant for three sites. However, average winter PDO was significantly correlated to growth only at the HL and ML sites. Correlations between growth and ENSO varied over previous and current years. Tree growth and January-March and April ENSO values had a positive relationship. Winter ENSO was significant for growth only at SC and HL, but spring ENSO had positive, significant correlations for SC, HL, and BL. Correlations between current year tree growth, PDO, and ENSO indicate that radial growth is higher during warm phases of these cycles and lower during cool phases. Patterns in PDO and ENSO correlations were consistent for all four sites. Correlations switched from negative to positive during the late spring and summer months of the previous growth year, and winter-month PDO and ENSO values had the most influence on growth.

Correlations between tree growth and climatic variables were also examined (Fig. 3, 4). Previous year July and August temperatures were negatively correlated with growth, and December temperature was positively correlated with current year growth. All four sites had similar patterns for correlations with temperature and previous and current year tree growth. Correlations switched from negative to positive during previous year summer months.

Correlations were significantly negative between February precipitation and growth at all four sites, and total winter precipitation and growth were negatively correlated for three sites. PDSI values for various winter months were negatively correlated to growth, and both April 1st snowpack depth and SWE were negatively correlated with tree growth, indicating that radial growth at the sampling sites is sensitive to precipitation during the winter months.

The same circulation variables were examined for correlations with net, winter, and summer mass balance (Fig. 5, 6). January, March, and April PNA were negatively correlated with net and winter balance, whereas July PNA was negatively correlated with summer and net balance. All balances had significant negative correlations with previous year June-September and current year October-April ENSO. Summer and net balance and ENSO also had a negative relationship during May. Winter and spring ENSO had significant negative correlations with all balances. Previous year August and September and current year October-June PDO values were significantly negatively correlated with both winter and net balances. Average winter and spring PDO index had a significant negative relationship with winter and net mass balance. Summer balance had no significant correlations with PDO for any previous or current year months. The results observed for PNA, ENSO, and PDO correlations suggest that these circulation indices influence mass balance similarly.

Mass balance measurements were correlated with several climatic variables (Fig. 6, 7). October-February precipitation had a positive relationship with winter and net balance, and total winter precipitation correlated significantly to all three balances. April 1st SWE was positively correlated with net, summer, and winter balances, and April 1st snowpack had positive correlations with net and winter balance. All three components of mass balance had a positive correlation with November-June PDSI, and net and summer balance had a positive correlation

with current year July-September PDSI values. Correlations with PDO, PDSI, precipitation, snowpack, and SWE indicate that net, winter, and sometimes summer balances are positively influenced by precipitation during the winter months. Temperatures in October, March, and April were correlated negatively with winter and net balance, and May and June temperatures were negatively correlated with net and summer balance.

South Cascade Glacier mass balance reconstruction

Principal components analysis produced four components. The first principal component (PC1) accounted for 67% of the variance among the four sampling sites. The second principal component explained only an additional 14% of the variance. Because PC1 explained so much of the variance in the chronologies, it was assumed to be a sufficient representation of the common growth variability in all sites.

Correlations between all site chronologies and PC1 and net balance were significant ($p<0.05$) (Fig. 8). All chronologies except SC had significant relationships with winter balance, and PC1, HL, and SC were correlated with summer balance.

The chronologies, including PC1, were used separately in a simple linear regression with net balance. The same procedure was also used with winter and summer mass balance values. Examination of model statistics and residuals revealed that all five regressions were significant ($p<0.05$) and could be used to reconstruct net mass balance, despite the relatively low R^2 values (Table 3). Site chronologies and PC1 were used to reconstruct net balance at SCG over the common period of 1659-2009. All chronologies produced reconstructions with comparable time periods of sustained above- and below-average mass balance (Fig. 9). This indicates that radial growth at each site is reacting to similar forcings and each site is reconstructing a similar

scenario of past mass balance. Although all reconstructions had comparable results, PC1 was chosen as the best reconstruction of net balance, because it displayed a common growth pattern among the four sampled sites. PC1 did not have the highest R^2 value, but it was thought to include both winter and summer balance signals. A 10-year moving average curve fit to the reconstruction (Fig. 10) highlights several extended periods of above-average net mass balance: 1690-1710, 1810-1820, 1845-1860, 1865-1890, and 1974-1990. Extended periods of below-average net mass balance include 1680-1690, 1790-1810, 1820-1840, and 1930-1960.

Winter balance had the highest correlation and R^2 value with the ML chronology and was reconstructed from its growth index (see Table 3). The ML chronology extended from 1615 to 2009. The winter balance reconstruction had many alternating periods of continued above- and below-average mass balance (Fig. 10). Prolonged positive mass balance occurred in 1630-1650, 1660-1680, 1695-1710, 1750-1760, 1785-1795, 1810-1820, 1845-1860, 1865-1890, and 1970-1985. Several of these periods of extended above-average winter balance are concurrent with periods of positive net balance. Sustained negative winter balance occurred in 1680-1700, 1720-1730, 1760-1775, 1790-1800, 1830-1845, 1890-1915, 1925-1955.

Summer balance was reconstructed from the HL chronology, which had the highest correlation and R^2 value (see Table 3, Fig. 10). The HL chronology dated from 1346 to 2009. Above-average summer mass balance occurred during 1395-1425, 1495-1510, 1580-1600, 1645-1660, 1690-1705, 1720-1765, 1810-1820, 1845-1905, and 1970-1990. Many periods of above-average summer balance coincide with decades of both positive winter and net balance. Below-average summer balance persisted during 1425-1455, 1550-1580, 1635-1645, 1680-1690, 1705-1720, 1765-1780, 1790-1805, 1820-1845, and 1920-1955.

Fig. 11 shows the reconstructed mass balance values plotted with the observed balance over the 50-year measurement period. This comparison highlights the ability of the chronologies to model the observations, which lends credibility to the assumption that tree growth is a feasible proxy for mass balance. The similarity in the modeled and observed values also increases confidence in viewing the reconstructed trends as a suitable representation of past balance. However, the model does not always perform well. The magnitude of the measured values is frequently underestimated, and as a result, years of extreme above- or below-average mass balance are often poorly modeled.

The reconstruction model also fails to capture the variability present in the observed record. Comparing the cumulative net mass balance of the observed and reconstructed values emphasizes its muted response (Fig. 12). The cumulative net balance of the observed record has more variability, while the reconstruction shows the cumulative balance to decline rather steadily. Examination of record statistics during the observation period (1959-2009), shows that the observed and reconstructed values have a similar mean and median, but that the reconstruction has a much lower standard deviation (Table 4). As in any regression, the variance of the fitted values is less than the variance of the observations.

DISCUSSION

Reconstructions of net, summer, and winter balance all have roughly the same time periods of above-average mass balance, mainly the early 1700s, 1810-1820, 1845-1860, 1865-1890, and 1970 to around 1990 (Fig. 10). Comparing these periods of positive mass balance to reconstructions of other glaciers in the PNW reveals similar results (Lewis and Smith 2004; Watson and Luckman 2004; Larocque and Smith 2005; Wood et al. 2011) (Fig. 13). All reconstructions, including this one, have common positive periods during 1695-1710, the 1810s and 1820s, 1860-1880, and the 1970s. Similar negative periods are 1790-1805, the 1820s-1840, and 1930-1950. The reconstructions used various tree species from many different locations around the PNW, and each reconstruction is for a different glacier or glaciers in the region as a whole, yet several periods of sustained above- and below-average mass balance are common, suggesting that glaciers in the PNW are responding to similar forcings. This indicates that these reconstructions may reflect a regional signal, at least for glaciers with similar topographic features.

Comparison to moraine dates from PNW studies also verifies the usefulness of our SCG reconstruction as a broad regional tool. Periods of positive mass balance should generally precede moraine dates. Heikkinen (1984) dated moraines for Coleman Glacier on Mount Baker (about 75 km from SCG) and found dates of around 1740, 1820, and 1855, late 1880s, 1910, 1920, and the late 1970s. These dates, especially those in the 1800s, fall just after periods of significant above-average mass balance from the reconstruction. Several studies have been done on moraine dates for glaciers in the Coast Mountains of British Columbia and the Canadian Rocky Mountains. In a record of moraine dates for 66 glaciers in the Canadian Rocky

Mountains, Luckman (2000) found that most glaciers experienced moraine-building periods in 1700-1725, 1825-1850, and 1850-1875. Larocque and Smith (2003) investigated moraine dates in the Mt. Waddington area of the Coast Mountains and found that many glaciers had moraine dates in 1770-1785, 1820-1840, 1870-1900, 1915-1930, and the mid 1940s. Koch et al. (2007) compared moraine dates for glaciers in Garibaldi Provincial Park, also in the southern Coast Mountains, and concluded that the most extensive moraine-building episode occurred during 1690-1720. The majority of these moraine dates occurred just after periods of notable positive mass balance as reconstructed for SCG (Fig. 14). However, this is a coarse-scale result, and differences in moraine dating techniques, local climates, and glacial dynamics complicate the comparison.

A few shorter-term reconstructions of mass balance at SCG have been created. Tangborn (1980) used monthly mean temperature and total precipitation records to model SCG mass balance from 1884 to 1974. Rasmussen (2009) reconstructed SCG mass balance from 1935 to 1958 from daily precipitation and temperature records, and he also adjusted the observed values from 1959 to 2006 to the 1970 constant-topography values. These net balance reconstructions had a few similar below-average periods, such as the 1940s, and above-average periods, the 1970s, as the net reconstruction in this study, although there are some disagreements, such as during 1910-1930 (Fig. 15). Even though reconstruction in this study appears muted and fails to capture the variability in these reconstructions, it does follow the patterns of the peaks and troughs. The cumulative net balance also shows the failure of our reconstruction to match the variability of these reconstructions (Fig. 15). Tangborn (1980) slightly underestimates the observed cumulative balance, and the Rasmussen (2009) reconstruction follows it closely until the early 1990s. Again, the reconstruction in this study does not do as well at fitting the

cumulative balance. The differences between these reconstructions may have been caused by the variables used in creating the model, such as temperature and precipitation records.

In their extensive study of glaciers in the PNW, Larocque and Smith (2005) reconstructed the winter balance of SCG from 1835 to 1999. They found periods of positive winter balance in 1860-1890, 1895-1900, 1910-1920, 1950-1965, and 1975-1985. The winter balance reconstructed in this study was above-average during the similar periods of 1865-1890 and 1970-1985. Negative balance was found in both reconstructions during the decades of the 1910s and 1940s. While there is some agreement between these two reconstructions, the discrepancies could be caused by reconstruction methods and the location of sampling sites used in the tree chronologies. Although this study used sites immediately surrounding SCG, Larocque and Smith (2005) used cores from further away that may have been responding to different local conditions.

Despite the overall agreement between the reconstruction in this study and those created in other studies in the PNW, our reconstruction seems to have a more dampened response than other glacial mass balance reconstructions. This could be due to a variety of differences among those studies and this one. Other studies have used an assortment of tree species (Engelmann spruce (*Picea engelmannii*), whitebark pine (*Pinus albicaulis*), Douglas-fir (*Pseudotsuga menziesii*)) from different locations, elevations, and aspects that might better correlate with mass balance changes, or the studies have used climate variables directly. Different chronology construction procedures have also been followed. Some studies used a double detrending method, and others chose not to prewhiten their chronologies with autoregressive models. Maximum latewood density chronologies have also been used to reconstruct mass balance rather than the tree-ring width chronologies created in this study. Even regression methods vary, with

some studies using two or more chronologies in a multiple regression to reconstruct mass balance.

The muted response of the reconstruction in this study could be due to any of the above reasons or combinations. It is possible that the sampling sites and trees chosen for this study did not suitably represent the climatic influences that are similar to those affecting SCG mass balance. The choice of detrending method and prewhitening could also be the cause of the dampened signal. Detrending is intended to remove tree age and growth characteristics, but in doing so, the low-frequency climate signal could have been affected. Prewhitening was done to remove the biological persistence in tree growth. Climate in one year influences growth directly in that year and also in successive years through energy storage. Removing this persistence could have removed growth trends related to climatic processes like ENSO or PDO. For example, the trees used in the chronologies could have experienced several consecutive years of above-average growth because ENSO was in its warm El Niño phase during this time. By prewhitening, the assumption was made that these years of growth were autocorrelated because of internal biological processes, rather than an external persistence force. Even though the reconstruction response is muted, the relationship between the growth chronology used in the reconstruction and the observed record was significant.

Correlations between PDO and ENSO indices and mass balance were examined in this study. Both PDO and ENSO had significant negative correlations with mass balance and positive correlations with tree growth (Fig. 2, 5). Warm phases of PDO and ENSO correspond to lower mass balance and higher tree radial growth, while increased mass balance and decreased growth occur during cool phases (Fig. 16). The reconstructed balances match the negative relationship found between the observed and index values, with a few small differences.

Correlations with PDO index were expected, as shown in other PNW glacier studies (Hodge et al. 1998; Bitz and Battisti 1999; Moore and Demuth 2001; Kovanen 2003; Lewis and Smith 2004; Pederson et al. 2004; Larocque and Smith 2005; Watson et al. 2006; Pelto 2008). However, this study also found that the ENSO index is significantly correlated with mass balance at SCG, despite the disagreement that exists in scientific literature (Hodge et al. 1998; Bitz and Battisti 1999; Moore and Demuth 2001 [weak correlation with ENSO]; Larocque and Smith 2005; Watson et al. 2006; Pelto 2008; Wood et al. 2011 [correlation with ENSO]). Several glacier mass balance studies in the PNW have shown that PNA primarily influences mass balance (Hodge et al. 1998; Bitz and Battisti 1999; Wood et al. 2011). Although significant correlations between mass balance and the PNA index were found in this study, the results suggest that ENSO has a strong relationship with all mass balance measurements at SCG and possibly has a stronger relationship than PNA.

Visual comparisons can be made with PDO and ENSO reconstructions to examine the relationship between these indices and mass balance in the past. Gedalof and Smith (2001b) reconstructed spring (March-May) PDO indices from mountain hemlock chronologies collected across coastal western North America. Periods of positive PDO index, such as 1680-1700, 1815-1840, 1920-1945, correspond with persistent negative mass balance in the reconstruction. Cool phases of the PDO reconstruction are similar to periods of positive mass balance in the early 1700s. A long period of variable PDO was found by Gedalof and Smith (2001b) for 1840-1923, whereas this study found that the mass balance reconstructions were consistently positive during most of that time. We visually compared the SCG reconstructed mass balance with the ENSO index created from a network of subtropical tree rings by D'Arrigo et al. (2005). The ENSO reconstruction is based on Niño-3 sea surface temperatures and is referred to as the Cook

reconstruction. The Cook reconstruction has warm phases (El Niño) that coincide with periods of notable negative mass balance as reconstructed in this study from 1790-1810 and around 1830-1850. Reconstructed cool phases (La Niña) during similar positive periods of mass balance were from 1660-1690, around 1850-1880, and 1960-80. Several periods of above- and below-average mass balance occurred during times that the Cook reconstruction predicted fairly stable ENSO values. Although the negative relationship between PDO, ENSO and mass balance seems to have existed in the past, there are times when this association fails. Comparing different reconstructions should be used for exploration and not as a definitive analysis.

Based on the moving average of the reconstructed values, the largest period of net mass balance was around 1700 and the lowest period was in the 1940s (Fig. 17). This low period in the 1940s occurred just after the widespread drought years of the 1930s, when SCG experienced prolonged high summer temperatures and low winter precipitation. Over the measurement record (1959-2009) the reconstruction was lowest in 2009, yet this low mass balance and a subsequent increase have occurred several times in the reconstruction period (Fig. 17). The observed record shows much lower mass balance for 2009, and although the reconstructed values are similar to the observed record, the reconstruction model does underestimate extreme values and does not clearly capture the magnitude and variability of the observed balance. For example, the reconstruction of net balance also shows a period of slight above-average mass balance from 1975 to the mid 1990s, but the observations recorded most of this time period as below-average balance. Both the reconstructed and observed values agree that a decline has taken place since the late 1990s.

Another way to analyze the recent decreasing trend in mass balance is to examine the rate of change from peaks of positive mass balance to the lowest point of negative balance. Rate of

change was calculated for several periods of time in which mass balance switched from positive to negative in the 10-year moving average of the reconstruction (Table 5). The 1940s were the period with the lowest mass balance in the reconstructed record, however the decline was gradual. The current decline from 2000 to 2009 in the reconstruction has the fastest rate in over a century. The closest rate of decrease to the observed values was around 1700, where the reconstruction shows the largest peak in net mass balance (Fig. 17).

According to the Office of the Washington State Climatologist, annual mean temperature at the Stehekin, Washington, station, around 25 kilometers from SCG, has increased by 0.12 degrees Celsius per decade during 1895-2010 (http://www.climate.washington.edu/trend analysis/). Mean annual temperature during 1895-1905 was 7.8 degrees Celsius, and during 2000-2010 mean annual temperature had increased to 9.0 degrees Celsius. Temperature in the twenty-first century is projected to increase, on average, 0.3 degrees Celsius per decade (Mote and Salathé 2010). Because of the negative relationship between temperature and mass balance, the increase in temperature can be expected to cause a decrease in mass balance. For the span of 2000-2009, SCG net mass balance averaged a decrease of 1.08 m w.e., while annual divisional temperatures increased an average of 0.06 degrees Celsius for the same time period. If temperatures do increase by 0.3 degrees Celsius per decade, SCG could experience an additional average decrease of approximately 5.40 m w.e per decade. This analysis is a result of several assumptions that need to be considered when stating this projection. The established relationship is between temperature and mass balance, not glacial extent (such as advance/retreat) which is complicated by underlying glacial ice flow dynamics (Cuffey and Paterson 2010). The relationship is also assumed to be directly linear, when in reality the connection between temperature and mass variation is complicated by other factors, such as the glacier's topographic

features. The projection is also restricted to temperature as the only variable, rather than accounting for precipitation, ENSO or PDO phase, or other environmental factors.

This simple analysis takes into account only a rise in temperatures because much of the current glacier recession is attributed to warming temperatures as opposed to altered precipitation (McCabe et al. 2000; Pederson et al. 2004; Rasmussen and Conway 2004; Watson and Luckman 2004; Pelto 2006). However, spring snow-covered area, snowpack, and snow-water equivalent are decreasing in the PNW in accordance with rising temperatures over the last 30-40 years (Mote et al. 2005; McCabe and Wolock 2010; Pederson et al. 2011). With less precipitation falling as snow, there will be less accumulation to prevent additional mass balance loss. The warmer conditions have also likely led to a weakening correlation between mass balance and PDO over the past two decades, and these changes could overwhelm the current observed negative relationship (Josberger et al. 2009). This seems to be the case, as the winter PDO index has been relatively stable around zero since 2000 before declining again, yet the mass balance has continued to decrease over this time period (Fig. 16). It appears that the recent decrease can be attributed to climate change, rather than the influence of climatic modes of variability.

There are around 700 glaciers covering 250 km^2 and yielding 800 million m^3 of runoff annually in the North Cascade Range (Post et al. 1971). The expected continued decline in glacier mass balance will affect water resources in the PNW because many streams are fed by this runoff. Glaciers influence water flow and quality on different temporal scales (Fountain and Tangborn 1985), but most attention is given to seasonal influences. Within the last 20-30 years, most glacier-fed streams in the PNW have experienced a decline in late summer flow, and with continued glacier retreat, this decline is expected to intensify (Moore and Demuth 2001; Stahl and Moore 2006; Moore et al. 2009; Nolin et al. 2010; Pelto 2011).

Glacial meltwater contributions to streamflow during low-flow periods like late summer are crucial for municipalities, agricultural irrigation systems, hydroelectric power plants, and terrestrial and aquatic wildlife. Changes in flow amount and timing will create challenges for water-use planning. Hydroelectric power plants can adjust to this change in streamflow by capturing water in reservoirs during peak flow and releasing stored water for power accordingly. Municipalities and agricultural industries can accommodate reductions in streamflow by focusing on conservation and water-use efficiency. Glacier retreat is expected to cause increases in stream temperature, changes in sediment flow, and decreased water quality (Moore et al. 2009). These will affect the habitat, reproduction, and food supply of aquatic organisms, and wildlife managers will be challenged to mitigate these changes.

Applying this information broadly could be beneficial to other glaciated regions in North America where a rapid decline in glacier mass is taking place. Comparisons of the SCG reconstruction with similar glacier reconstructions and moraine dates in the PNW provides several periods of synchronous positive and negative mass balance. This indicates that SCG has responded in kind with other glaciers in the past and is a good indicator of regional glacier behavior. These comparable fluctuations in mass balance point to large-scale external climate forcings driving PNW glacier mass. SCG and other glaciers in the region have undergone several periods of sustained above- and below-average balance and several instances where mass balance was at equilibrium. SCG has recovered from similar low mass balance periods like the one experienced in the last decade, but the rate of this decline is faster than it has been in a century. If this trend continues and increases in magnitude, the PNW can expect to experience changes in glacier-influenced water resources.

REFERENCES

Bidlake, W.R., E.G. Josberger, and M.E. Savoca. 2010. Modeled and measured glacier change and related glaciological, hydrological, and meteorological conditions at South Cascade Glacier, Washington, balance and water years 2006 and 2007. U.S. Geological Survey Scientific Investigations Report 2010-5143. 82 p.

Bitz, C. M. and D. S. Battisti. 1999. Interannual to decadal variability in climate and the glacier mass balance in Washington, western Canada, and Alaska. Journal of Climate **12**:3181-3196.

Burbank, D. W. 1982. Correlations of climate, mass balances, and glacial fluctuations at Mount Rainier, Washington, USA, since 1850. Arctic and Alpine Research **14**:137-148.

Cook, E. R., and R. L. Holmes. 1996. Guide for computer program ARSTAN. Pages 75–87 in H. D. Grissino-Mayer, R. L. Holmes, and H. C. Fritts, editors. The international tree-ring data bank program library version 2.0 user's manual. University of Arizona, Tucson, Arizona, U.S.A.

Cuffey, K.M., and W.S.B. Paterson. 2010. The physics of glaciers. 4th ed. Elsevier, Inc.

D'Arrigo, R., E. R. Cook, R. J. Wilson, R. Allan, and M. E. Mann. 2005. On the variability of ENSO over the past six centuries. Geophysical Research Letters **32**, L03711, doi: 10.1029/2004/GL022055.

Dyurgerov, M. B. and M. F. Meier. 1999. Analysis of winter and summer glacier mass balances. Geografiska Annaler Series A-Physical Geography **81A**:541-554.

Fountain, A. G., M. J. Hoffman, F. Granshaw, and J. Riedel. 2009. The 'benchmark glacier' concept - does it work? Lessons from the North Cascade Range, USA. Annals of

Glaciology **50**:163-168.

Fountain, A. G. and W. V. Tangborn. 1985. The effect of glaciers on streamflow variations. Water Resources Research **21**:579-586.

Fritts, H. C. 1976. Tree rings and climate. Academic Press, London, UK.

Gedalof, Z. and D. J. Smith. 2001a. Dendroclimatic response of mountain hemlock (Tsuga mertensiana) in Pacific North America. Canadian Journal of Forest Research **31**:322-332.

Gedalof, Z. and D. J. Smith. 2001b. Interdecadal climate variability and regime-scale shifts in Pacific North America. Geophysical Research Letters **28**:1515-1518.

Granshaw, F. D. and A. G. Fountain. 2006. Glacier change (1958-1998) in the North Cascades National Park Complex, Washington, USA. Journal of Glaciology **52**:251-256.

Heikkinen, O. 1984. Dendrochronological evidence of variations of Coleman Glacier, Mount Baker, Washington, USA. Arctic and Alpine Research **16**:53-64.

Hodge, S. M., D. C. Trabant, R. M. Krimmel, T. A. Heinrichs, R. S. March, and E. G. Josberger. 1998. Climate variations and changes in mass of three glaciers in western North America. Journal of Climate **11**:2161-2179.

Holmes, R. L. 1983. Computer assisted quality control in tree-ring dating and measurement. Tree-Ring Bulletin **43**:69–78.

Josberger, E.G., W.R. Bidlake, R.S. March, and S. O'Neel. 2009. Fifty-year record of glacier change reveals shifting climate in the Pacific Northwest and Alaska, USA: U.S. Geological Survey Fact Sheet 2009-3046. 4 p.

Koch, J., J. J. Clague, and G. D. Osborn. 2007. Glacier fluctuations during the past millennium in Garibaldi Provincial Park, southern Coast Mountains, British Columbia. Canadian Journal of Earth Sciences **44**:1215-1233.

Koch, J., B. Menounos, and J. J. Clague. 2009. Glacier change in Garibaldi Provincial Park, southern Coast Mountains, British Columbia, since the Little Ice Age. Global and Planetary Change **66**:161-178.

Kovanen, D. J. 2003. Decadal variability in climate and glacier fluctuations on Mt Baker, Washington, USA. Geografiska Annaler Series A-Physical Geography **85A**:43-55.

Larocque, S. J. and D. J. Smith. 2003. Little Ice Age glacial activity in the Mt. Waddington area, British Columbia Coast Mountains, Canada. Canadian Journal of Earth Sciences **40**:1413-1436.

Larocque, S. J. and D. J. Smith. 2005. 'Little Ice Age' proxy glacier mass balance records reconstructed from tree rings in the Mt Waddington area, British Columbia Coast Mountains, Canada. The Holocene **15**:748-757.

Lewis, D. and D. Smith. 2004. Dendrochronological mass balance reconstruction, Strathcona Provincial Park, Vancouver Island, British Columbia, Canada. Arctic Antarctic and Alpine Research **36**:598-606.

Luckman, B. H. 2000. The Little Ice Age in the Canadian Rockies. Geomorphology **32**:357-384.

Mantua, N. J., S. R. Hare, Y. Zhang, J. M. Wallace, and R. C. Francis. 1997. A Pacific interdecadal climate oscillation with impacts on salmon production. Bulletin of the American Meteorological Society **78**:1069-1079.

McCabe, G. J. and A. G. Fountain. 1995. Relations between atmospheric circulation and mass-balance at South Cascade Glacier, Washington, USA. Arctic and Alpine Research **27**:226-233.

McCabe, G. J., A. G. Fountain, and M. Dyurgerov. 2000. Variability in winter mass balance of Northern Hemisphere glaciers and relations with atmospheric circulation. Arctic

Antarctic and Alpine Research **32**:64-72.

McCabe, G. J. and D. M. Wolock. 2010. Long-term variability in Northern Hemisphere snow cover and associations with warmer winters. Climatic Change **99**:141-153.

Meier, M. F., M. B. Dyurgerov, and G. J. McCabe. 2003. The health of glaciers: Recent changes in glacier regime. Climatic Change **59**:123-135.

Moore, R. D. and M. N. Demuth. 2001. Mass balance and streamflow variability at Place Glacier, Canada, in relation to recent climate fluctuations. Hydrological Processes **15**:3473-3486.

Moore, R. D., S. W. Fleming, B. Menounos, R. Wheate, A. Fountain, K. Stahl, K. Holm, and M. Jakob. 2009. Glacier change in western North America: influences on hydrology, geomorphic hazards and water quality. Hydrological Processes **23**:42-61.

Mote, P. W., A. F. Hamlet, M. P. Clark, and D. P. Lettenmaier. 2005. Declining mountain snowpack in western north America. Bulletin of the American Meteorological Society **86**:39-49.

Mote, P. W. and E. P. Salathé. 2010. Future climate in the Pacific Northwest. Climatic Change **102**:29-50.

Nolin A.P., J. Phillippe, A. Jefferson, and S.L. Lewis. 2010. Present-day and future contributions of glacier runoff to summertime flows in a Pacific Northwest watershed: implications for water resources. Water Resources Research **46**, W12409, doi: 10.1029/2009WR008968.

Oerlemans, J., B. Anderson, A. Hubbard, P. Huybrechts, T. Johannesson, W. H. Knap, M. Schmeits, A. P. Stroeven, R. S. W. van de Wal, J. Wallinga, and Z. Zuo. 1998. Modelling the response of glaciers to climate warming. Climate Dynamics **14**:267-274.

Pederson, G. T., D. B. Fagre, S. T. Gray, and L. J. Graumlich. 2004. Decadal-scale climate

drivers for glacial dynamics in Glacier National Park, Montana, USA. Geophysical Research Letters **31**, L12203, doi: 10.129/2004GL019770.

Pederson, G. T., S. T. Gray, C. A. Woodhouse, J. L. Betancourt, D. B. Fagre, J. S. Littell, E. Watson, B. H. Luckman, and L. J. Graumlich. 2011. The unusual nature of recent snowpack declines in the North American Cordillera. Science **333**: 332-335, doi: 10.1126/science.121570.

Pelto, M. S. 2006. The current disequilibrium of North Cascade glaciers. Hydrological Processes **20**:769-779.

Pelto, M. S. 2008. Glacier annual balance measurement, forecasting and climate correlations, North Cascades, Washington 1984-2006. Cryosphere **2**:13-21.

Pelto, M.S. 2011. Skykomish River, Washington: impact of ongoing glacier retreat on streamflow. Hydrological Processes **25**: 3356-3363.

Peterson, D. W. and D. L. Peterson. 2001. Mountain hemlock growth responds to climatic variability at annual and decadal time scales. Ecology **82**:3330-3345.

Phillips, E. L. 1965. Climate of Washington. In Climates of the States. Government Printing Office, Washington, D.C., USA.

Post, A., D. Richardson, W.V. Tangborn and F.L. Rosselot. 1971. Inventory of glaciers in The North Cascades, Washington. US Geological Survey Prof. Paper, 705-A. Washington, D.C.

R Development Core Team (2010). R: A language and environment for statistical computing. R Foundation for Statistical Computing, Vienna, Austria. ISBN 3-900051-07-0, URL http://www.R-project.org.

Rasmussen, L. A. 2009. South Cascade Glacier mass balance, 1935-2006. Annals of Glaciology

50:215-220.

Rasmussen, L. A. and H. Conway. 2001. Estimating South Cascade Glacier (Washington, USA) mass balance from a distant radiosonde and comparison with Blue Glacier. Journal of Glaciology **47**:579-588.

Rasmussen, L. A. and H. Conway. 2003. Using upper-air conditions to estimate South Cascade Glacier (Washington, USA) summer balance. Journal of Glaciology **49**:456-462.

Rasmussen, L. A. and H. Conway. 2004. Climate and glacier variability in western North America. Journal of Climate **17**:1804-1815.

Rasmussen, L. A. and R. M. Krimmel. 1999. Using vertical aerial photography to estimate mass balance at a point. Geografiska Annaler Series a-Physical Geography **81A**:725-733.

Rasmusson, E. M. and J.M. Wallace. 1983. Meteorological aspects of the El Niño/Southern Oscillation. *Science*, **222**, 1195-1202.

Shea, J. M. and S. J. Marshall. 2007. Atmospheric flow indices, regional climate, and glacier mass balance in the Canadian Rocky Mountains. International Journal of Climatology **27**:233-247.

Sitts, D. J., A. G. Fountain, and M. J. Hoffman. 2010. Twentieth century glacier change on Mount Adams, Washington, USA. Northwest Science **84**:378-385.

Stahl, K. and R. D. Moore. 2006. Influence of watershed glacier coverage on summer streamflow in British Columbia, Canada. Water Resources Research **42**, W06201, doi:10.129/2006WR05022.

Stokes, M. A., and T. L. Smiley. 1968. An introduction to tree-ring dating. University of Arizona Press, Tucson, Arizona, USA.

Tangborn, W. 1980. 2 models for estimating climate-glacier relationships in the North Cascades,

Washington, USA. Journal of Glaciology **25**:3-21.

Tangborn, W. 1999. A mass balance model that uses low-altitude meteorological observations and the area-altitude distribution of a glacier. Geografiska Annaler Series a-Physical Geography **81A**:753-765.

Walters, R.A. and M.F. Meier. 1989. Variability of glacier mass balances in western North America. In Peterson, D.H. (ed.), Aspects of Climate Variability in the Pacific and Western Americas. Geophsical Monograph Series 55: 365-374. American Geophysical Union, Washington D.C.

Watson, E. and B. H. Luckman. 2004. Tree-ring-based mass-balance estimates for the past 300 years at Peyto Glacier, Alberta, Canada. Quaternary Research **62**:9-18.

Watson, E., B. H. Luckman, and B. Yu. 2006. Long-term relationships between reconstructed seasonal mass balance at Peyto Glacier, Canada, and Pacific sea surface temperatures. Holocene **16**:783-790.

Wood, L.J., D.J. Smith, and M.N Demuth. 2011. Extending the Place Glacier mass-balance record to AD 1585, using tree rings and wood density. Quaternary Research **76**:305-313.

Table 1: A summary of site and tree characteristics. Mean DBH represents the average diameter of breast height for trees at each site, and SD is the standard deviation in the diameter.

Site	Mean elevation (m)	Longitude	Latitude	Mean DBH (SD) (cm)	Year range	Median age (yr)	Mean age (yr)
Hidden Lake (HL)	1769	-121.208797	48.5047562	51.7 (5.7)	1346-2011	371	385
South Cascade (SC)	1613	-121.078867	48.3736037	76.8 (12.6)	1392-2011	349	367
Bagley Lakes (BL)	1297	-121.685031	48.8606919	68.6 (8.1)	1659-2011	298	302
Minotaur Lake (ML)	1703	-121.035864	47.8443795	51.3 (8.6)	1615-2011	296	293

Table 2: Summary of chronology statistics. Series mean first-order autocorrelation and mean interseries correlation values are prior to autoregressive modeling. Mean sensitivity values are calculated after autoregressive modeling.

Site	n	Series mean first-order autocorrelation	Mean interseries correlation (r_{avg})	Mean sensitivity	Autoregressive order	Autoregressive R^2
Hidden Lake	17	0.480	0.294	0.231	4	0.24
South Cascade	17	0.371	0.318	0.186	2	0.15
Bagley Lakes	19	0.386	0.299	0.191	2	0.17
Minotaur Lake	18	0.549	0.307	0.191	2	0.33

Table 3: Summary of regression statistics for each site and mass balance. Correlations (r) are significant ($p<0.05$) at the threshold value of $r = 0.28$. All R^2 listed are significant ($p<0.05$). Regression models have normal, independent residuals.

	South Cascade Glacier mass balance								
Site	Net balance			Summer balance			Winter balance		
	r	R^2	Equation	r	R^2	Equation	r	R^2	Equation
Hidden Lake	-0.47	0.22	$y = 2.497 - 3.157x$	-0.42	0.18	$y = -1.494 - 1.878x$	-0.29	0.08	$y = 3.990 - 1.279x$
South Cascade	-0.33	0.11	$y = 1.326 - 1.966x$	-0.32	0.10	$y = -2.091 - 1.271x$	-0.18	NS	-
Bagley Lakes	-0.31	0.09	$y = 1.352 - 1.964x$	-0.13	NS	-	-0.33	0.11	$y = 4.134 - 1.412x$
Minotaur Lake	-0.37	0.14	$y = 1.826 - 2.455x$	-0.15	NS	-	-0.41	0.17	$y = 4.519 - 1.810x$
PC1	0.43	0.18	$y = -0.626 + 1.616x$	0.30	0.09	$y = -3.345 + 0.740x$	0.35	0.13	$y = 2.720 + 0.875x$

Table 4: Summary of mass balance reconstruction statistics compared to observed balance statistics.

	Net balance		Winter balance		Summer balance	
	Reconstructed	Observed	Reconstructed	Observed	Reconstructed	Observed
Mean	-0.59	-0.59	2.74	2.74	-3.33	-3.33
Median	-0.62	-0.69	2.74	2.60	-3.31	-3.34
Standard Deviation	0.42	0.97	0.26	0.64	0.27	0.64
Sum	-29.91	-29.91	139.79	139.79	-169.70	-169.70

Table 5: Rates of change for periods of decreasing net mass balance in the reconstructed and observed record.

Reconstructed Net Balance			Observed Net Balance		
Time range	Years	Rate of change (m w.e/yr)	Time range	Years	Rate of change (m w.e/yr)
1700-1710	10	-0.055	1976-1988	12	-0.080
1790-1800	10	-0.038	2000-2009	9	-0.062
1815-1831	16	-0.029			
1856-1863	7	-0.036			
1883-1892	9	-0.040			
1924-1947	23	-0.016			
1976-1988	12	-0.010			
2000-2009	9	-0.031			

FIGURES

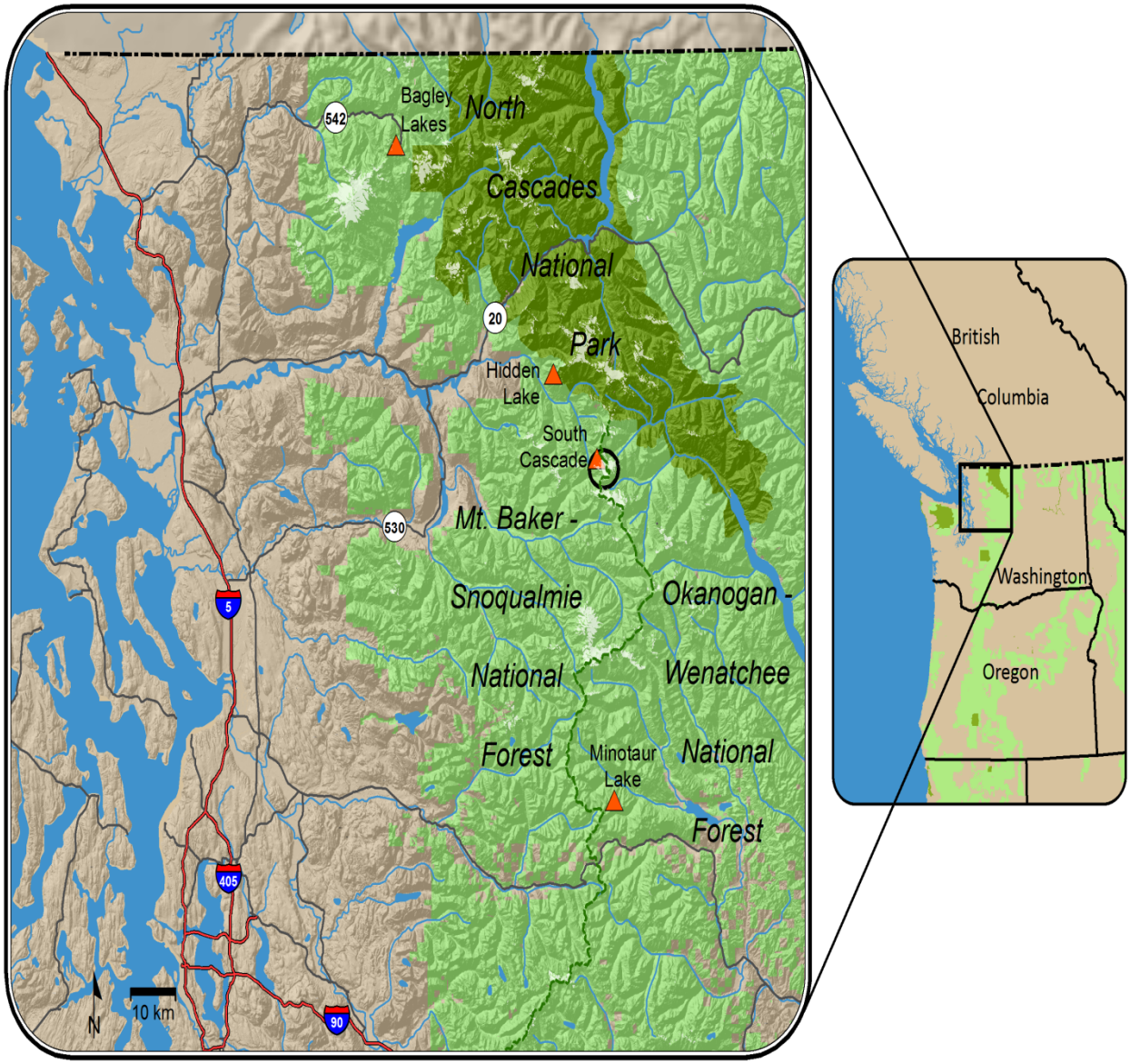

Figure 1: Map of sampling sites. Orange triangles represent sampling locations. Black circle represents the location of South Cascade Glacier. Shaded light green areas represent National Forests, and shaded dark green areas are National Parks.

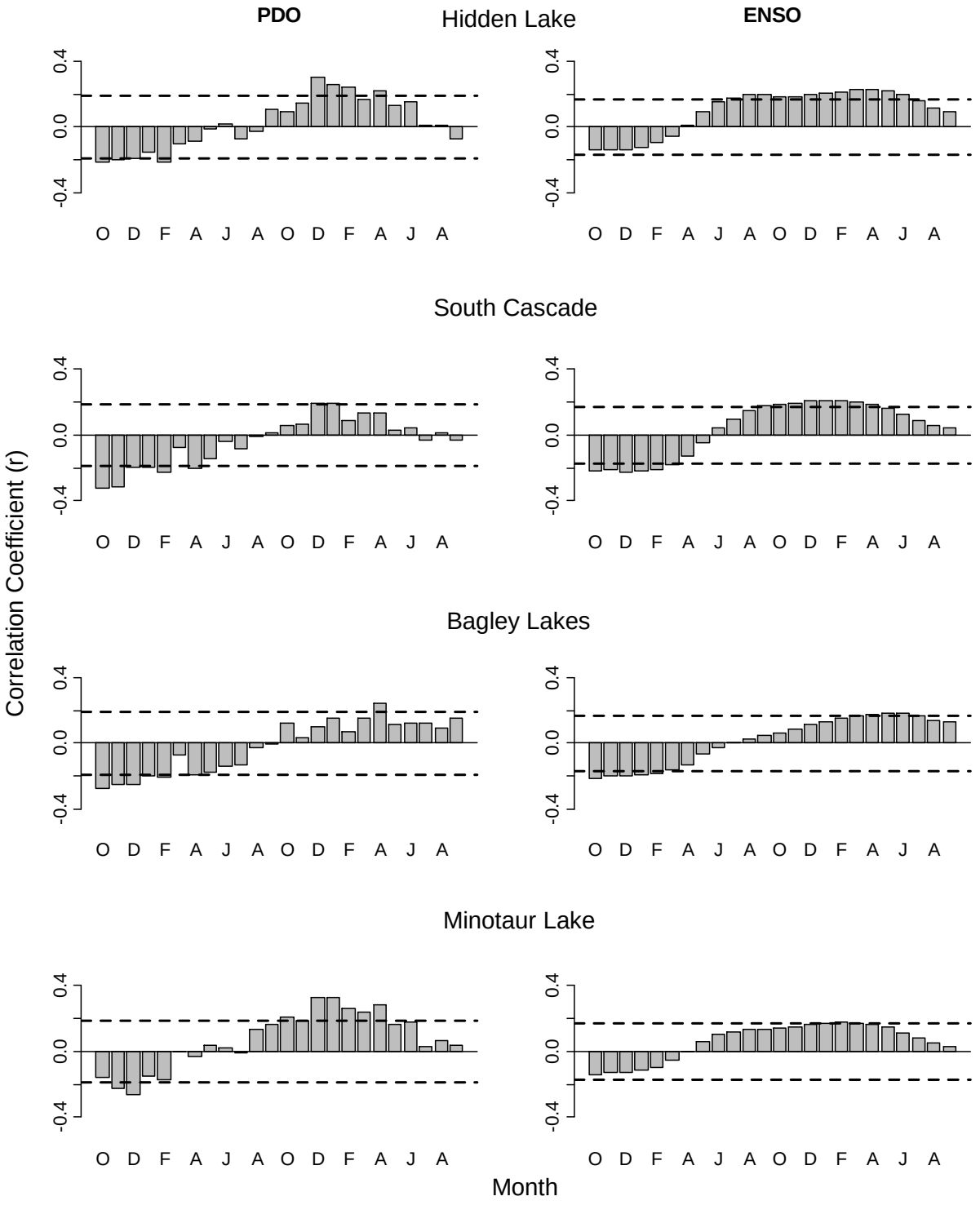

Figure 2: Correlations (r) between mountain hemlock growth and the Pacific Decadal Oscillation index (PDO) and the Niño 3.4 index (ENSO). Dashed lines indicate a significance ($p<0.05$) cut-off of $r = 0.19$ (PDO) and $r = 0.17$ (ENSO).

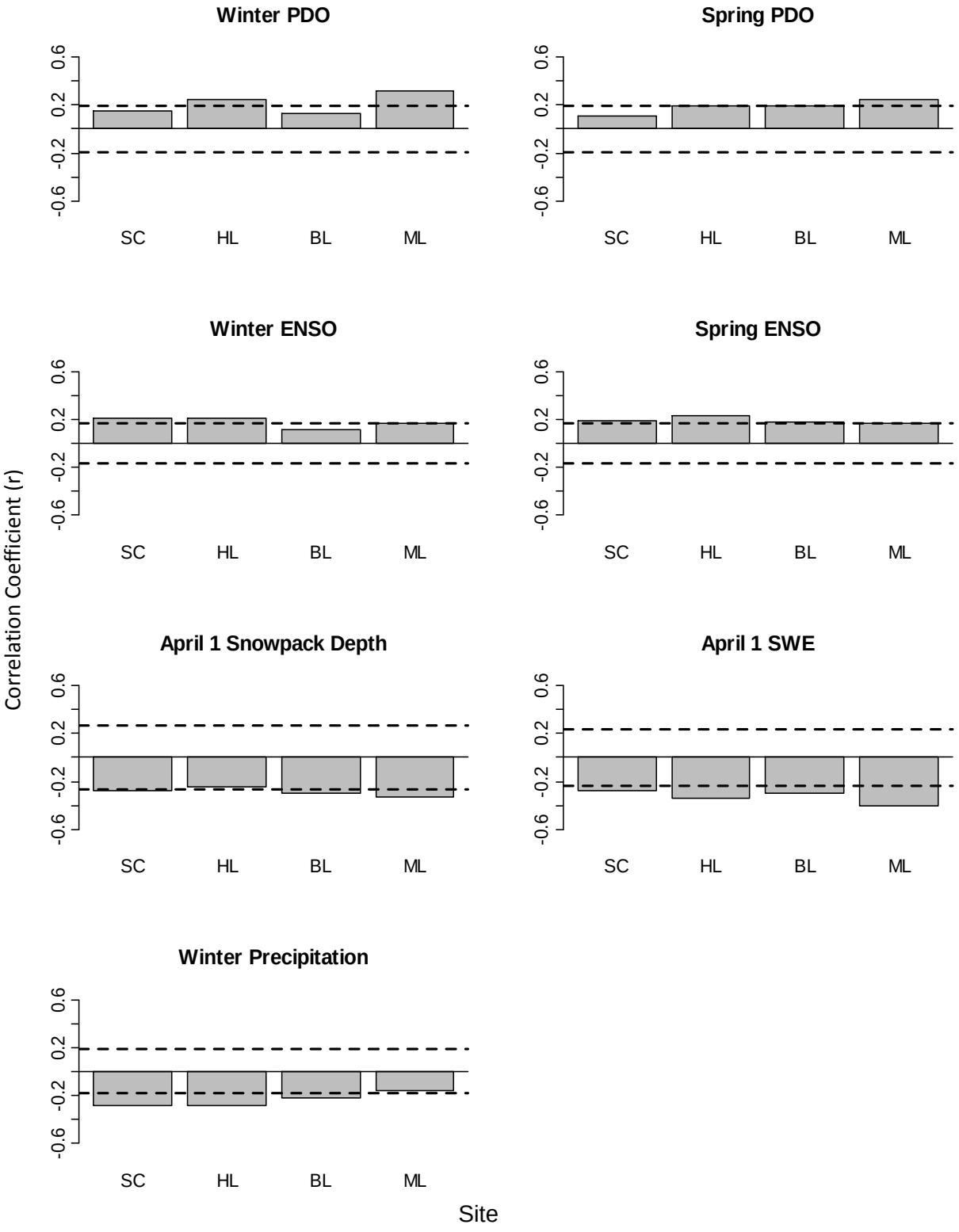

Figure 3: Correlations (r) between mountain hemlock growth and winter (October-March) and summer (March-May) Pacific Decadal Oscillation index (PDO), Niño 3.4 index (ENSO), and total monthly precipitation, and April 1 snowpack depth and snow-water-equivalent (SWE). Dashed lines indicate a significance ($p<0.05$) cut-off of r = 0.19 (PDO), r = 0.17 (ENSO), r=0.18 (precipitation), r=0.27 (snowpack depth), and r=0.23 (SWE).

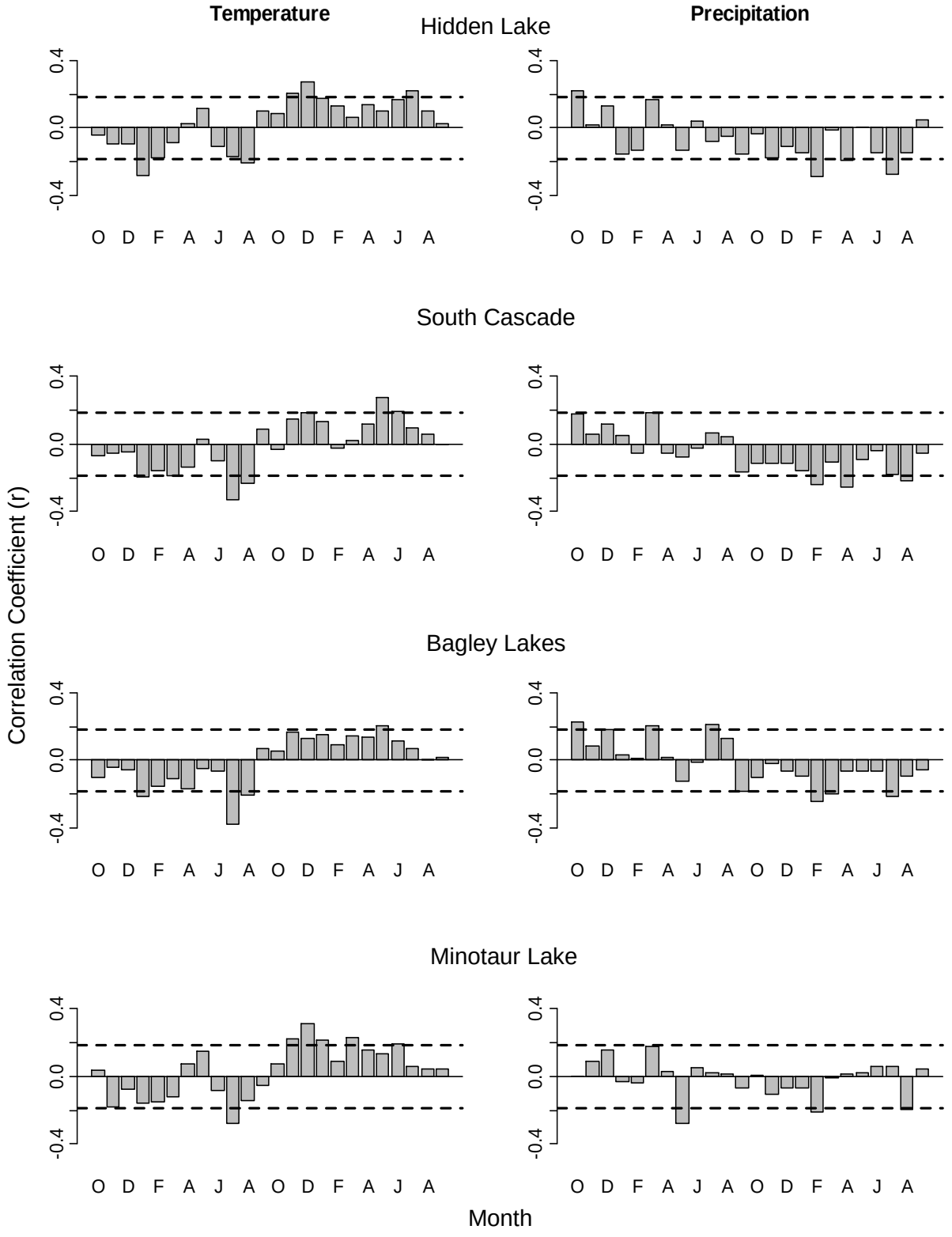

Figure 4: Correlations (r) between mountain hemlock growth and divisional monthly average temperature and total monthly precipitation. Dashed lines indicate a significance ($p<0.05$) cut-off of $r = 0.19$.

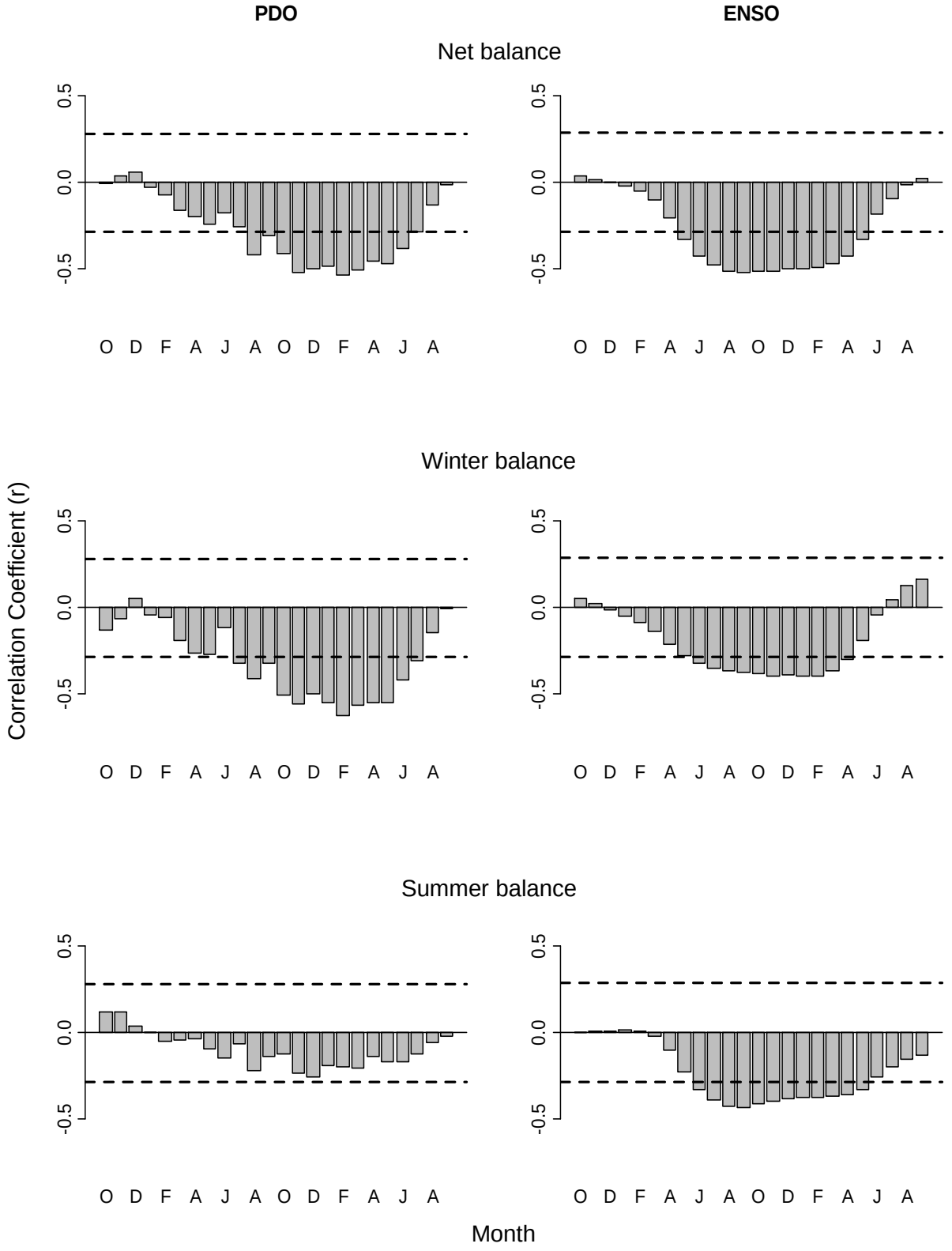

Figure 5: Correlations (r) between observed mass balance and the Pacific Decadal Oscillation index (PDO) and the Niño 3.4 index (ENSO). Dashed lines indicate a significance ($p<0.05$) cut-off of $r = 0.28$ (PDO) and $r = 0.29$ (ENSO).

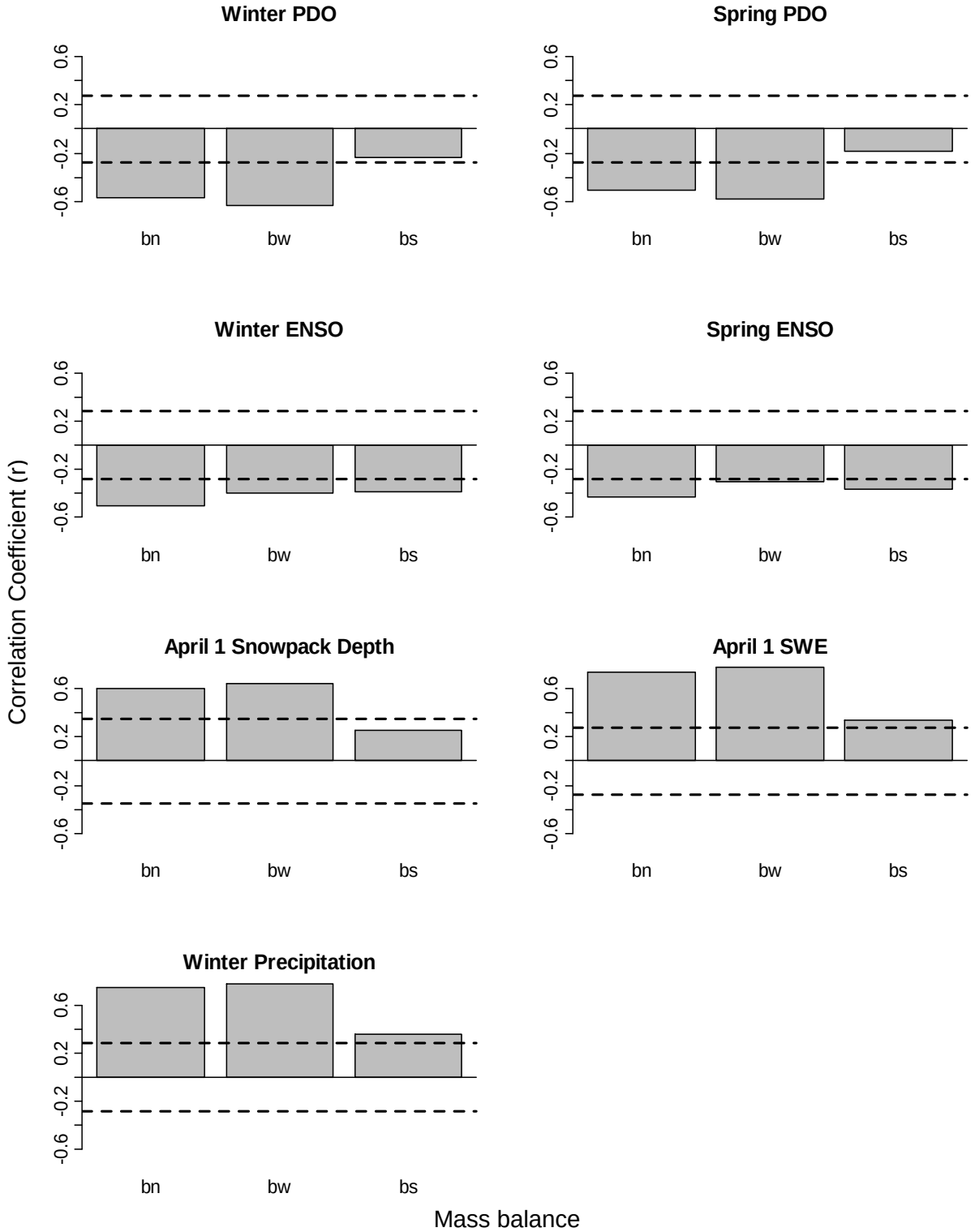

Figure 6: Correlations (r) between observed mass balance and winter (October-March) and summer (March-May) Pacific Decadal Oscillation index (PDO), Niño 3.4 index (ENSO), and total monthly precipitation, and April 1 snowpack depth and snow-water-equivalent (SWE). Net balance is designated bn, winter as bw, and summer is bs. Dashed lines indicate a significance ($p<0.05$) cut-off of $r = 0.28$ (PDO, SWE, precipitation), $r = 0.29$ (ENSO), and $r=0.35$ (snowpack depth).

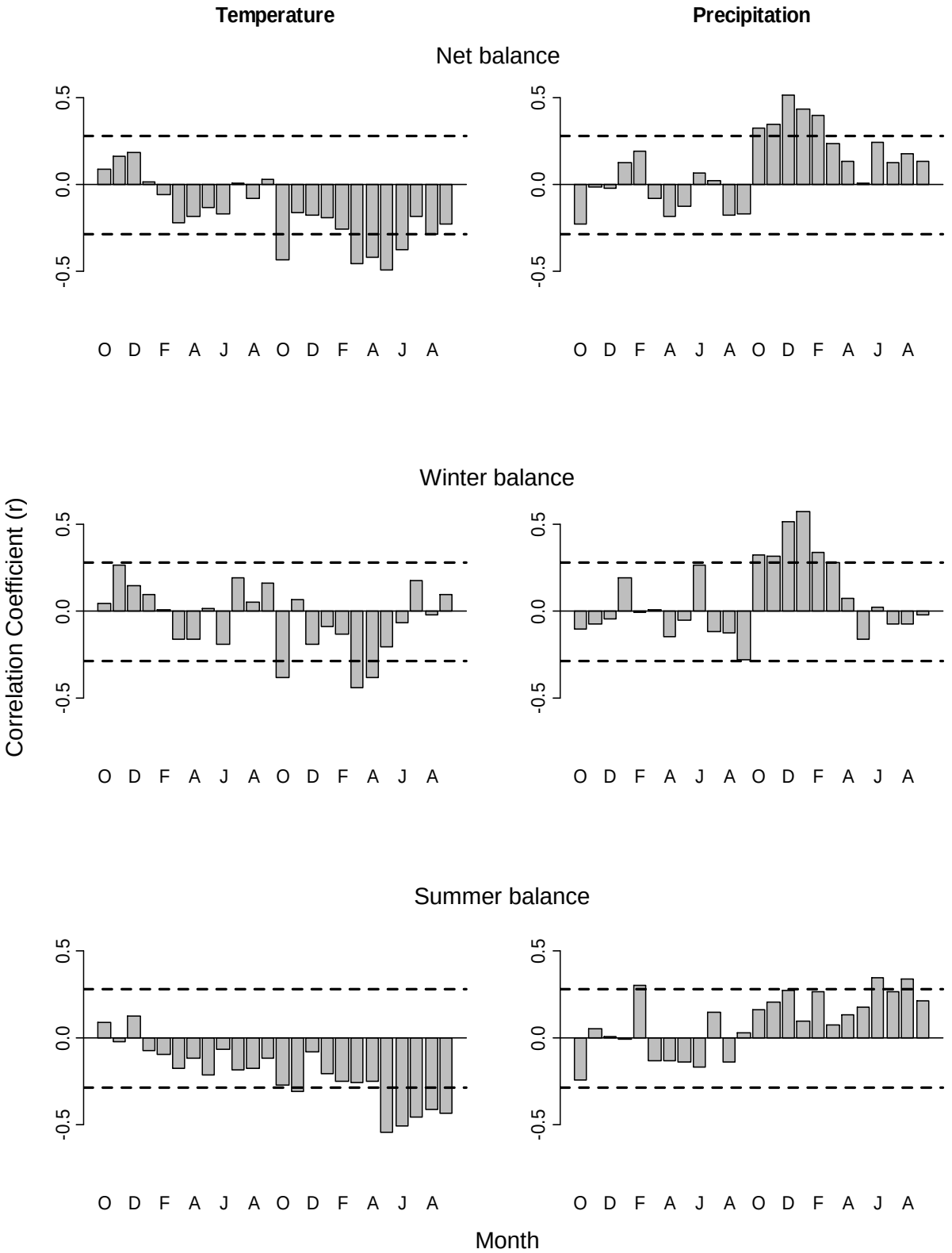

Figure 7: Correlations (r) between observed mass balance and divisional monthly average temperature and total monthly precipitation. Dashed lines indicate a significance ($p<0.05$) cut-off of $r = 0.28$.

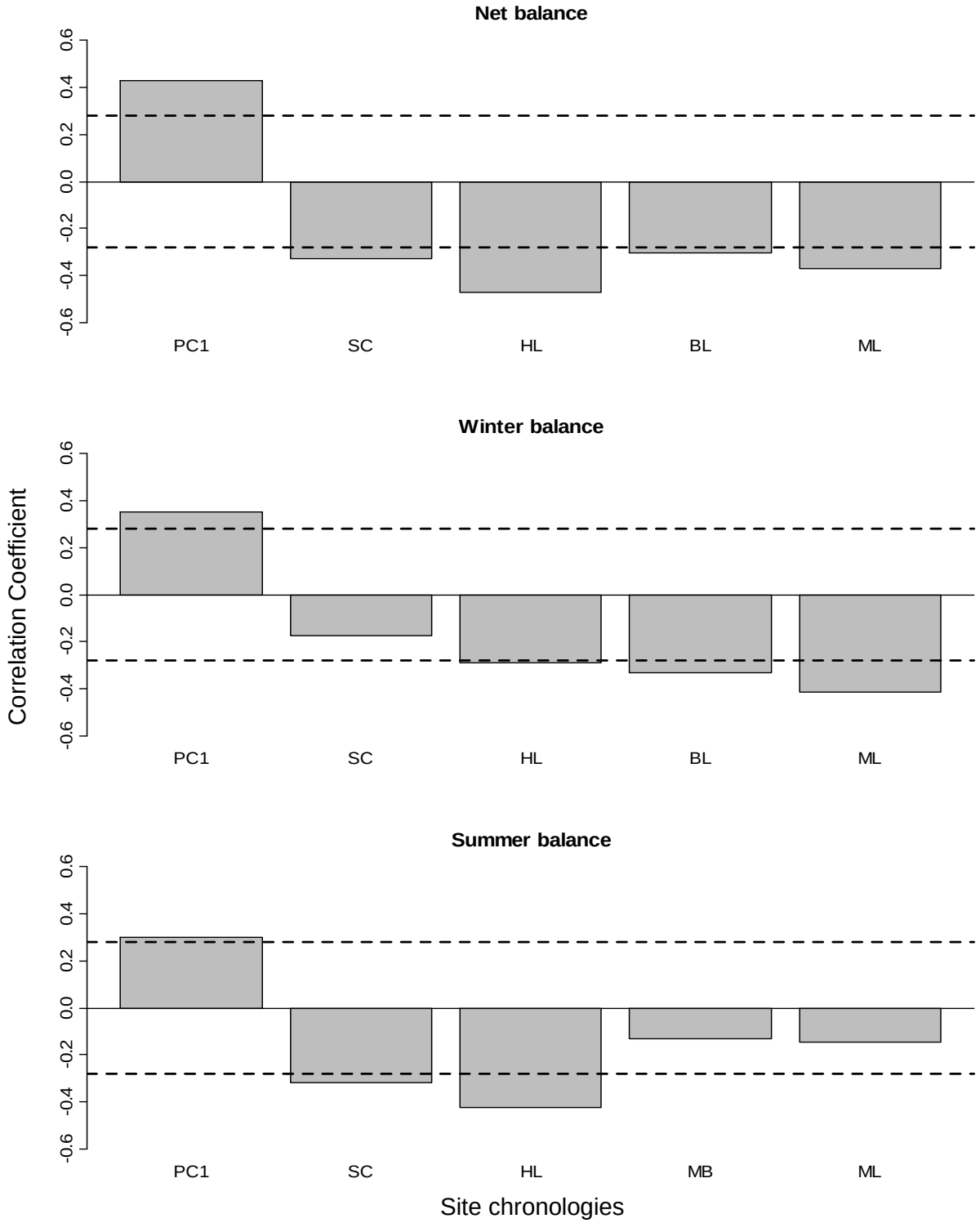

Figure 8: Correlations (r) between mountain hemlock residual site chronologies (PC1, South Cascade, Hidden Lake, Bagley Lakes, and Minotaur Lake) and mass balance values for the measurement period of 1959-2009. Dashed lines indicate significance threshold of $r = 0.28$ ($p<0.05$). The growth chronologies at all four sites have a negative relationship with mass balance, and PC1 has a positive relationship. Principal components analysis transforms, reduces, and compiles the original data, and as a result of these changes, correlations with PC1 are different from correlations with the site chronologies.

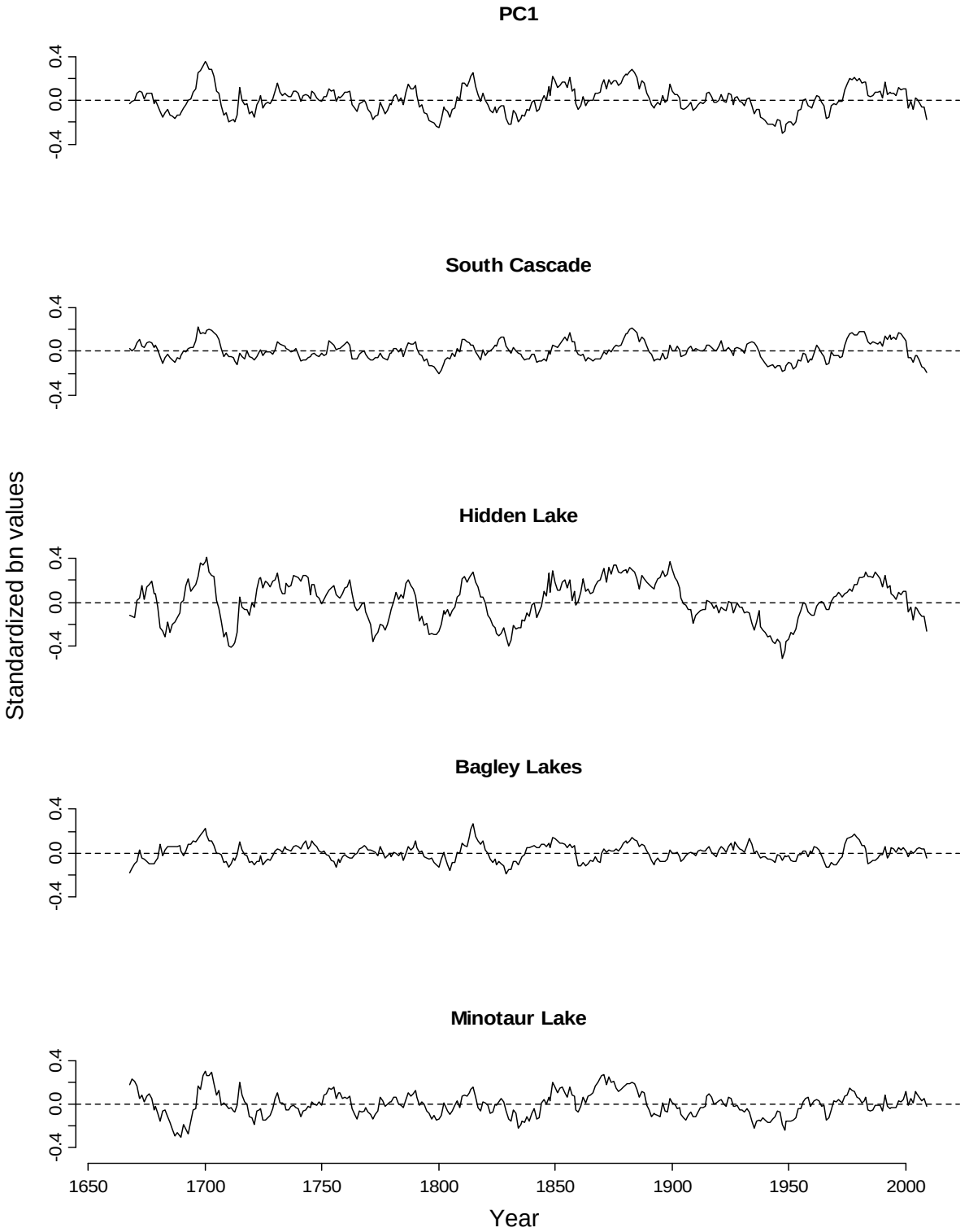

Figure 9: Time series plots of net balance reconstructions over the common span 1659-2009. The solid lines represent a moving average of 10 years. The moving average helps identify similar peaks and troughs in net balance among the five reconstructions. The reconstructions of mass balance were standardized by adding in the mean of the reconstruction in order to show a clearer picture of periods of above or below average balance.

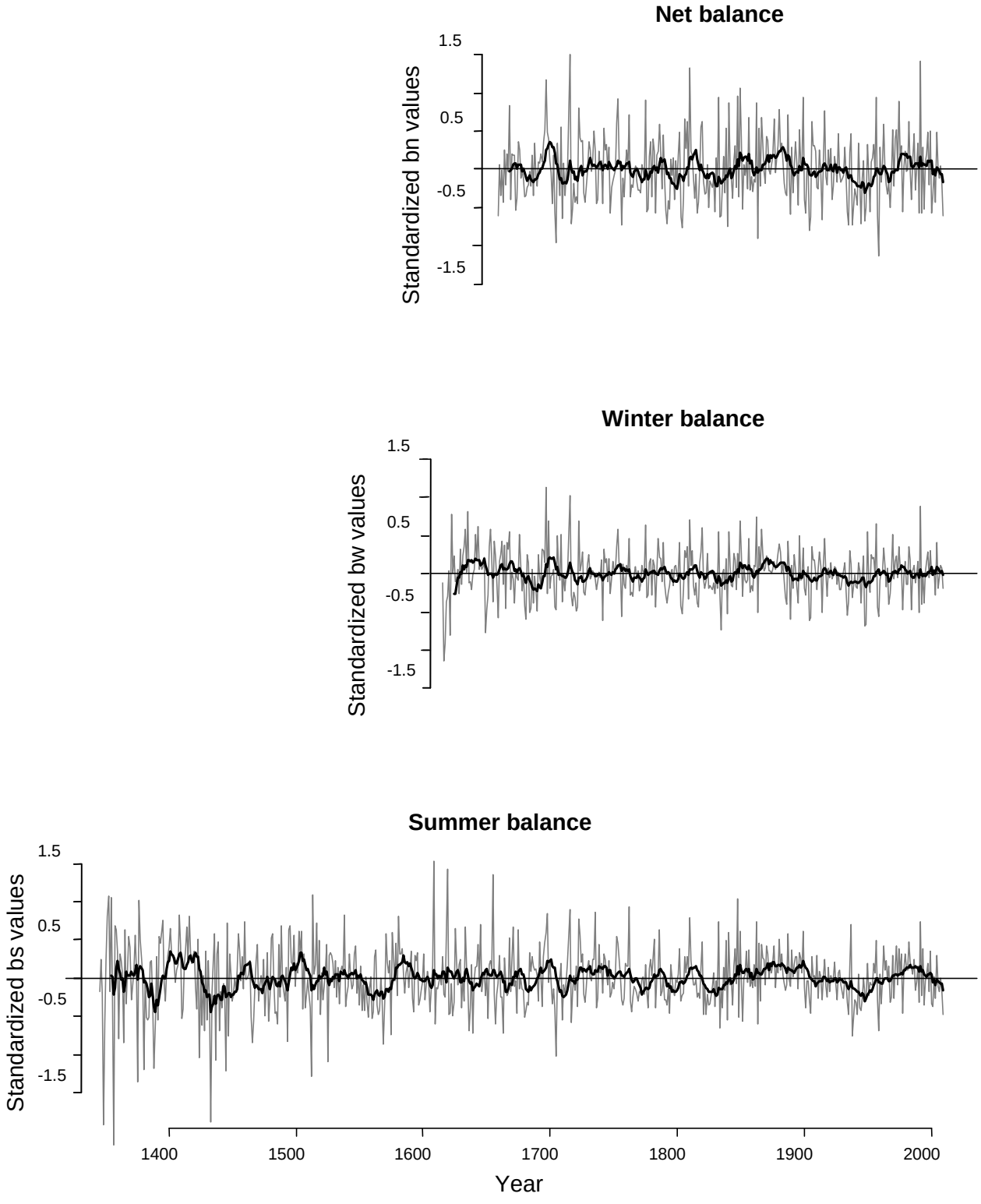

Figure 10: Time series plots of reconstruction net, winter, and summer mass balance. Net balance is reconstructed from PC1 for 1659-2009, winter balance is reconstructed from the Minotaur Lake residual chronology for the span 1615-2009, and summer balance is reconstructed from the Hidden Lake residual chronology, 1346-2009. The thick black line represents a 10-year moving average.

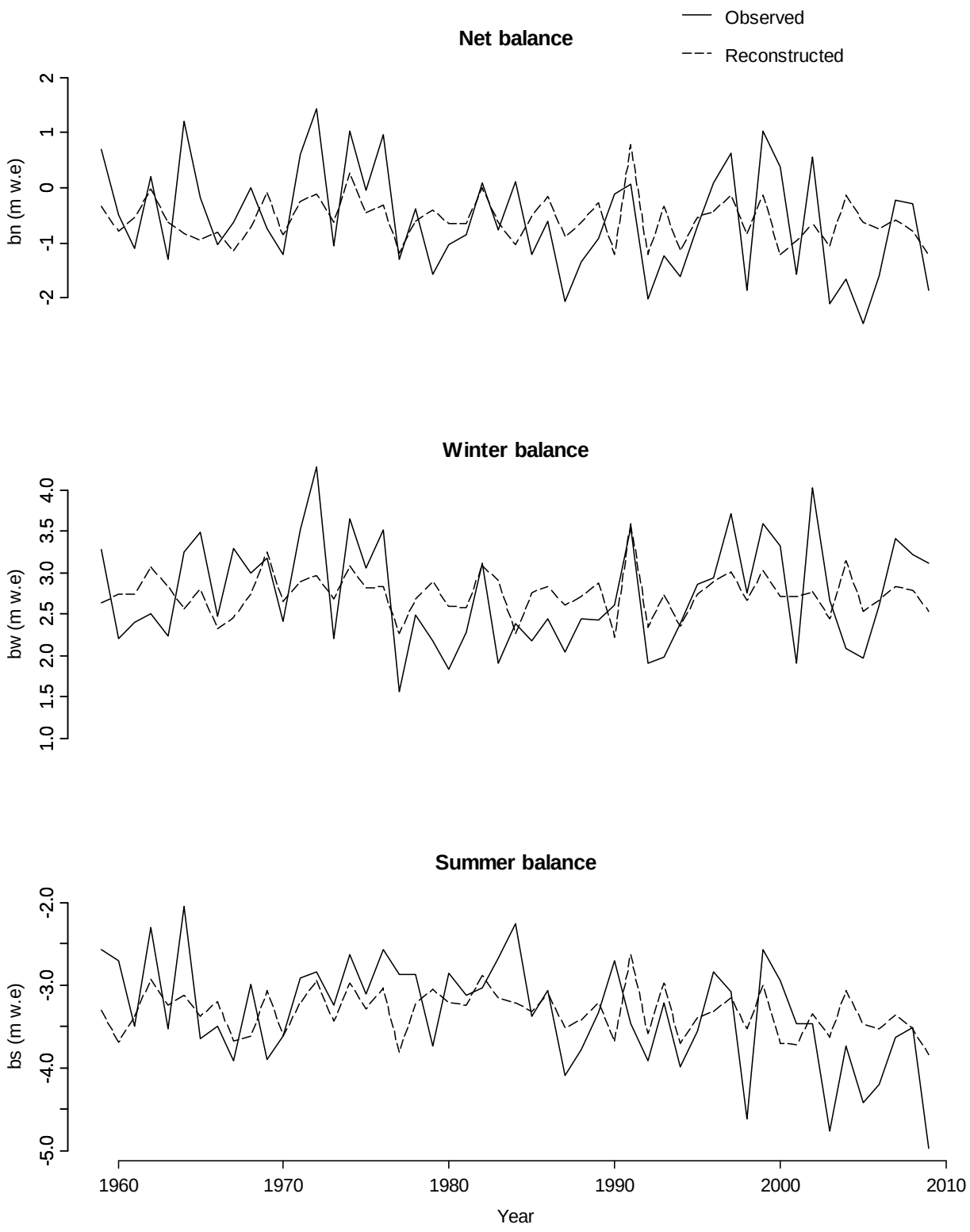

Figure 11: Fitted mass balance (dashed line) plotted against the observed balance values (solid line) for the measurement period of 1959-2009. Net balance is fitted from PC1, winter balance is from the Minotaur Lake residual chronology, and summer balance used the Hidden Lake residual chronology.

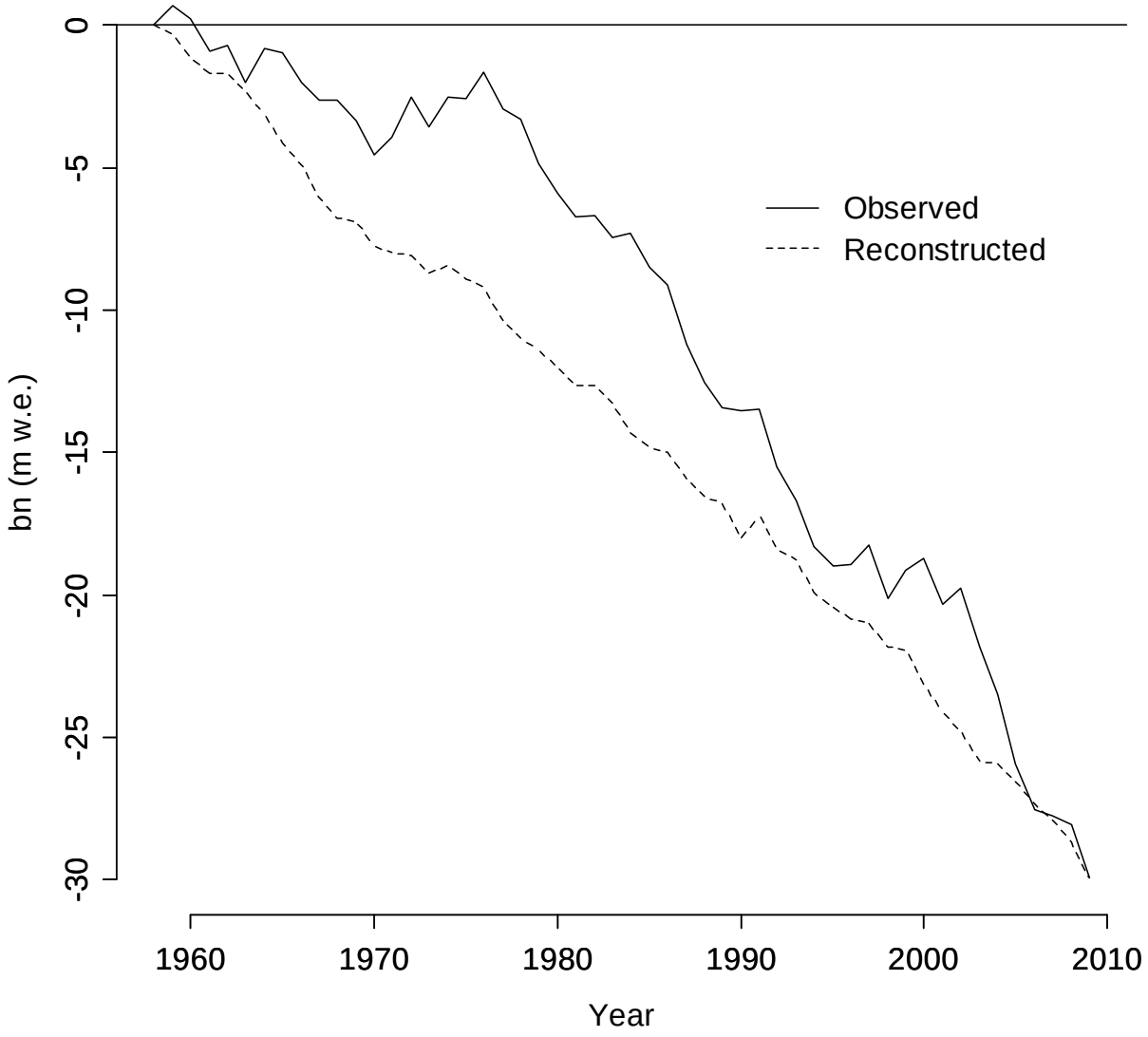

Figure 12: Comparison of reconstructed and observed cumulative net mass balance over the observation period, 1959-2009

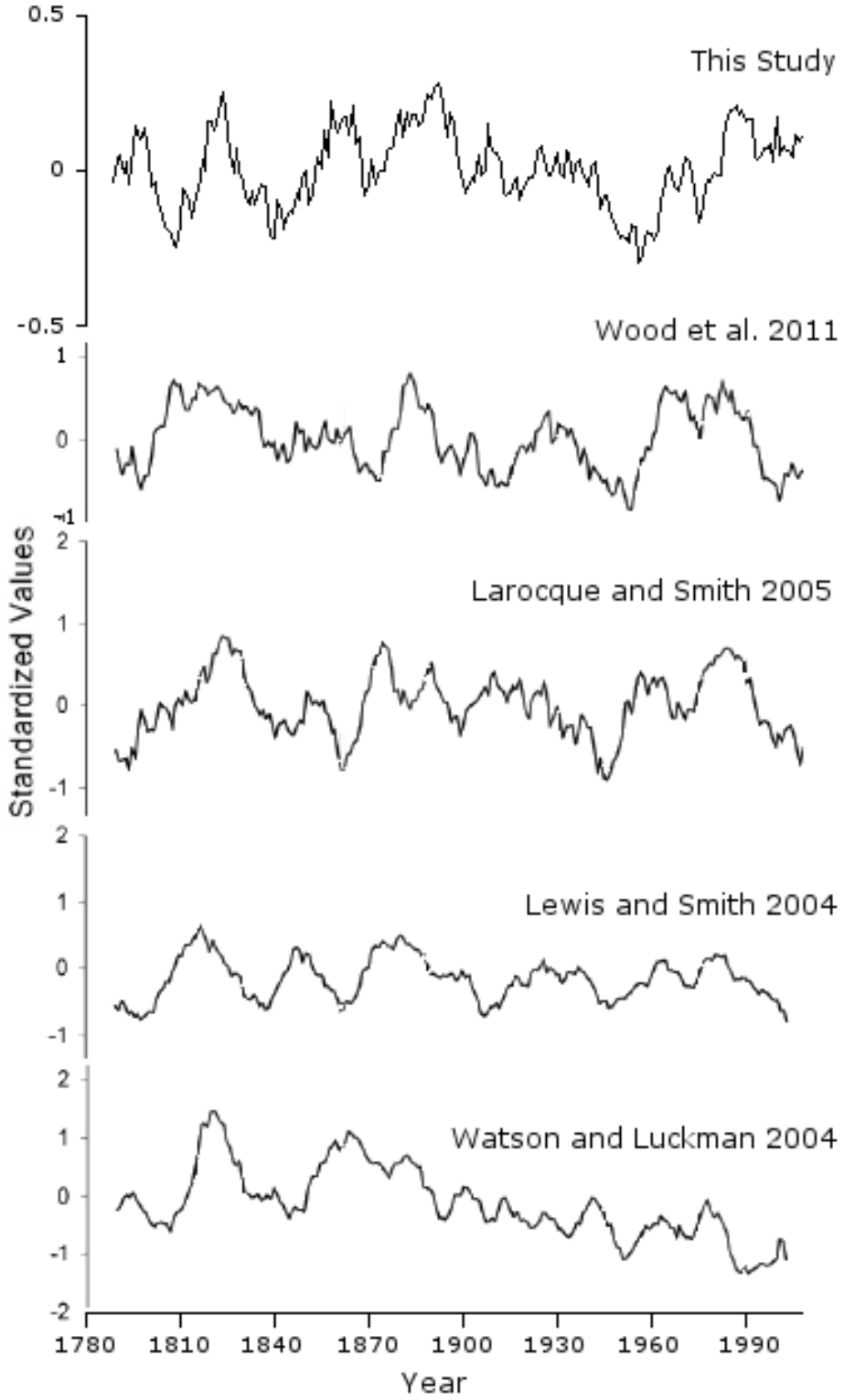

Figure 13: Comparison of the reconstructed net balance created in this study to reconstructed net balance created in similar studies in the Pacific Northwest. Adapted from Wood et al. 2011.

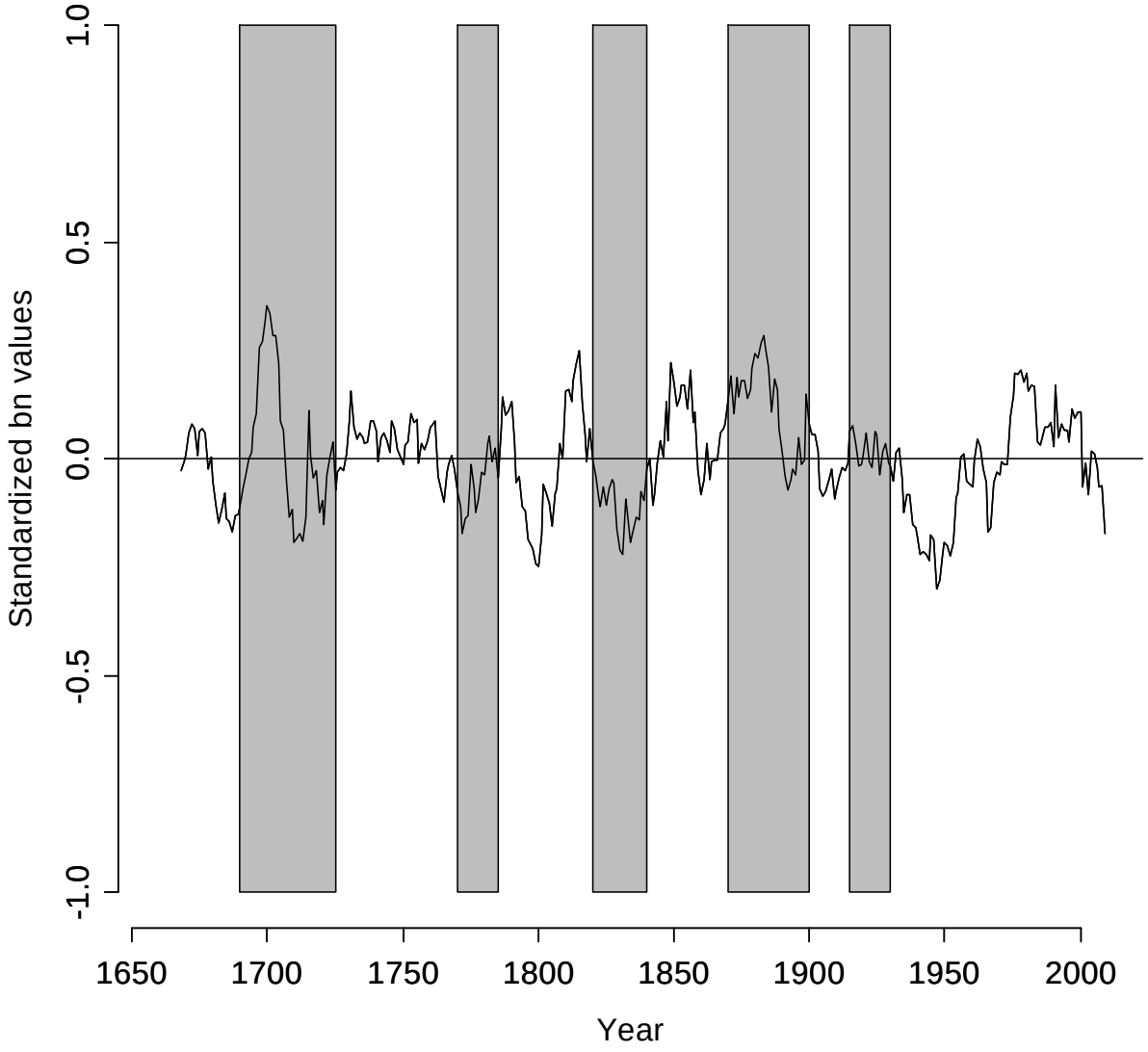

Figure 14: Time series plot of the 10-year moving average of the reconstructed net balance. The shaded rectangles represent compilations of moraine dates in the Pacific Northwest (Heikkinen 1984; Luckman 2000; Larocque and Smith 2003; Koch et al. 2007). Periods of notable above-average mass balance took place during, or just before, these broadly dated time periods.

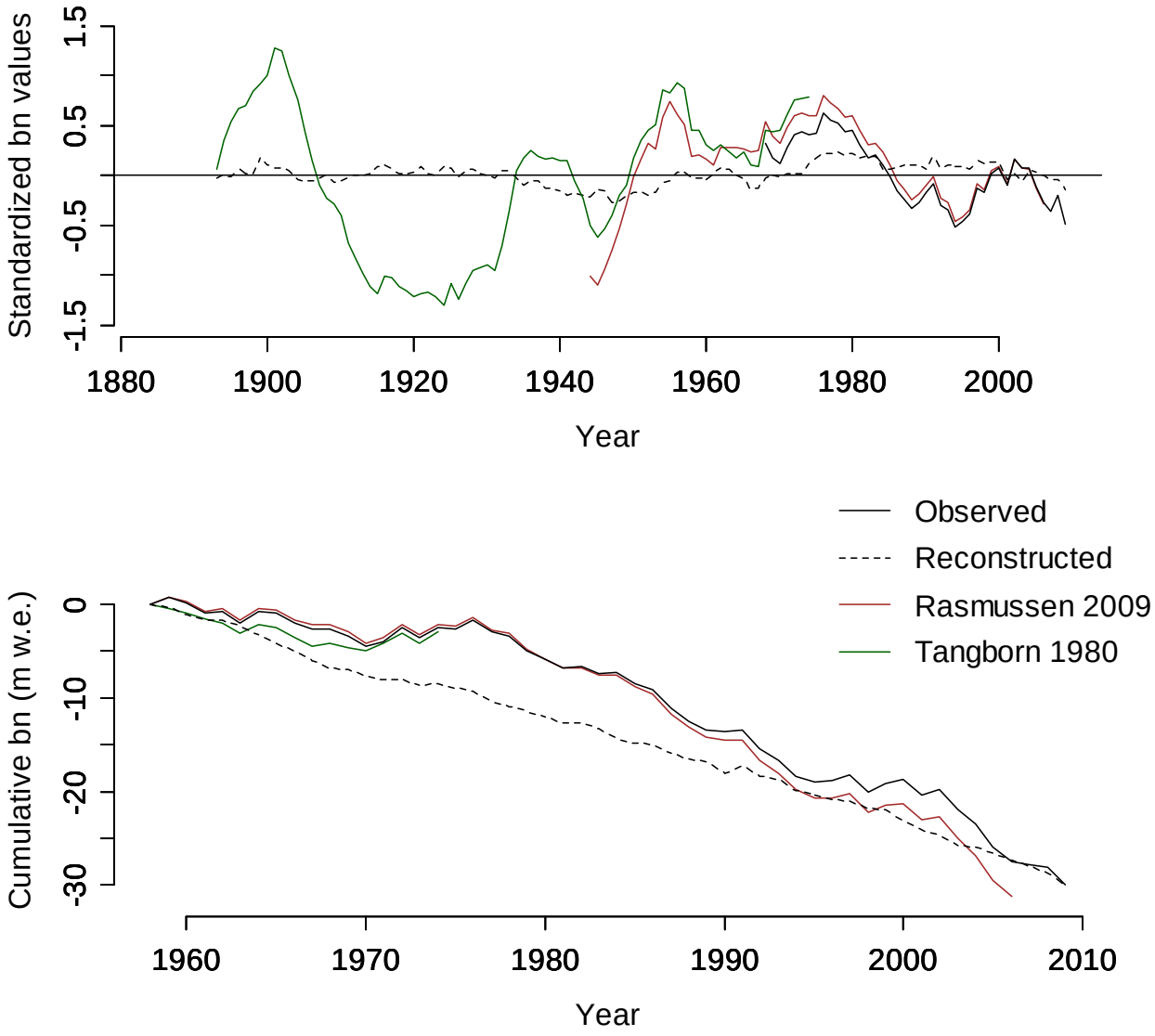

Figure 15: The top graph represents time series plots comparing net balance reconstructions for South Cascade Glacier. The solid black line represents the observed balance, the dashed black line is the reconstructed net balance from this study, the solid brown line is reconstructed net balance from Rasmussen (2009), and the solid green line is reconstructed balance taken from Tangborn (1980). The bottom graph is a comparison of the cumulative net balance during the observation period, 1959-2009.

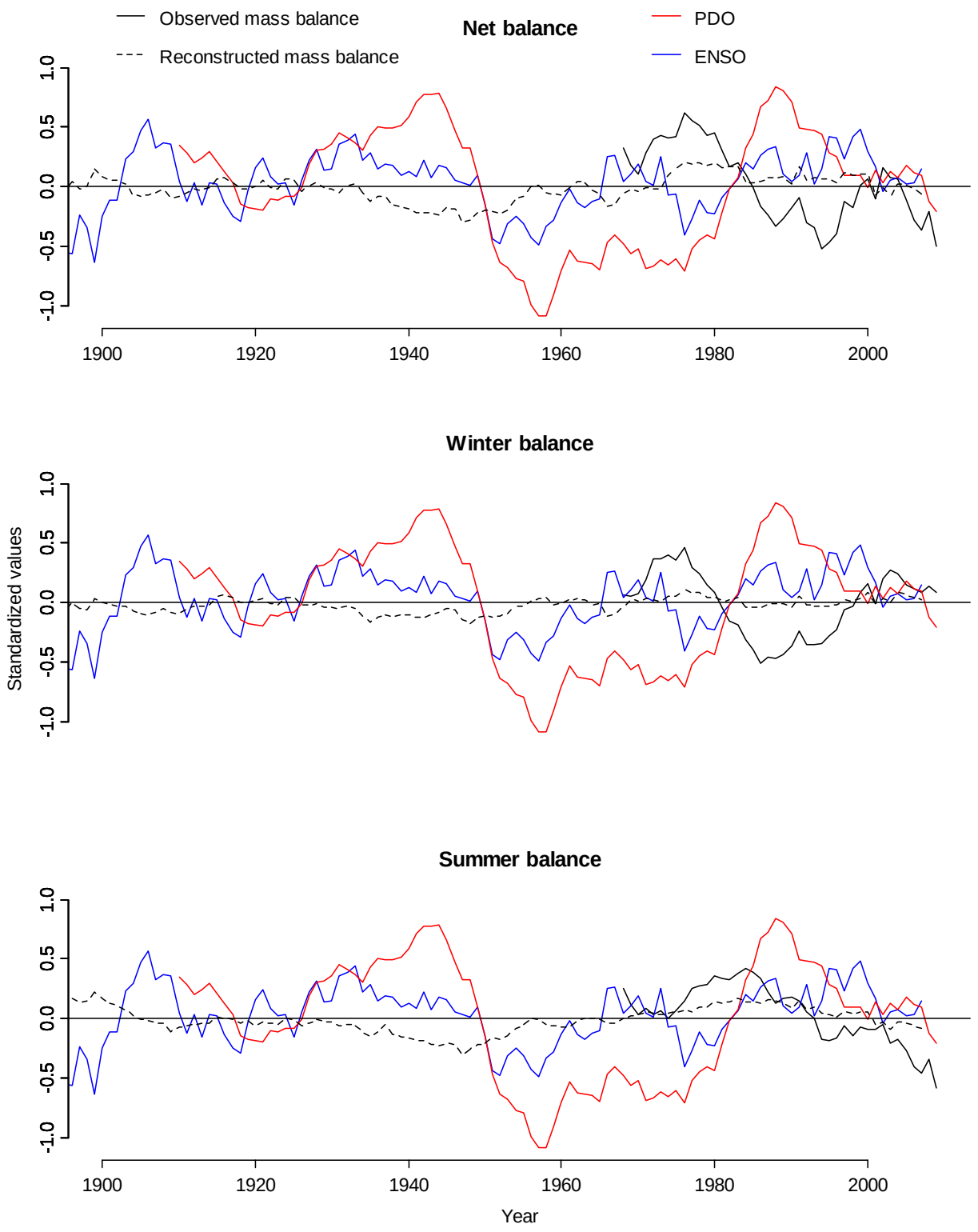

Figure 16: Time series plots of reconstructed mass balance, observed mass balance, average winter Pacific Decadal Oscillation (PDO) index values, and average winter Niño 3.4 (ENSO) index. These series are displayed as a 10-year moving average.

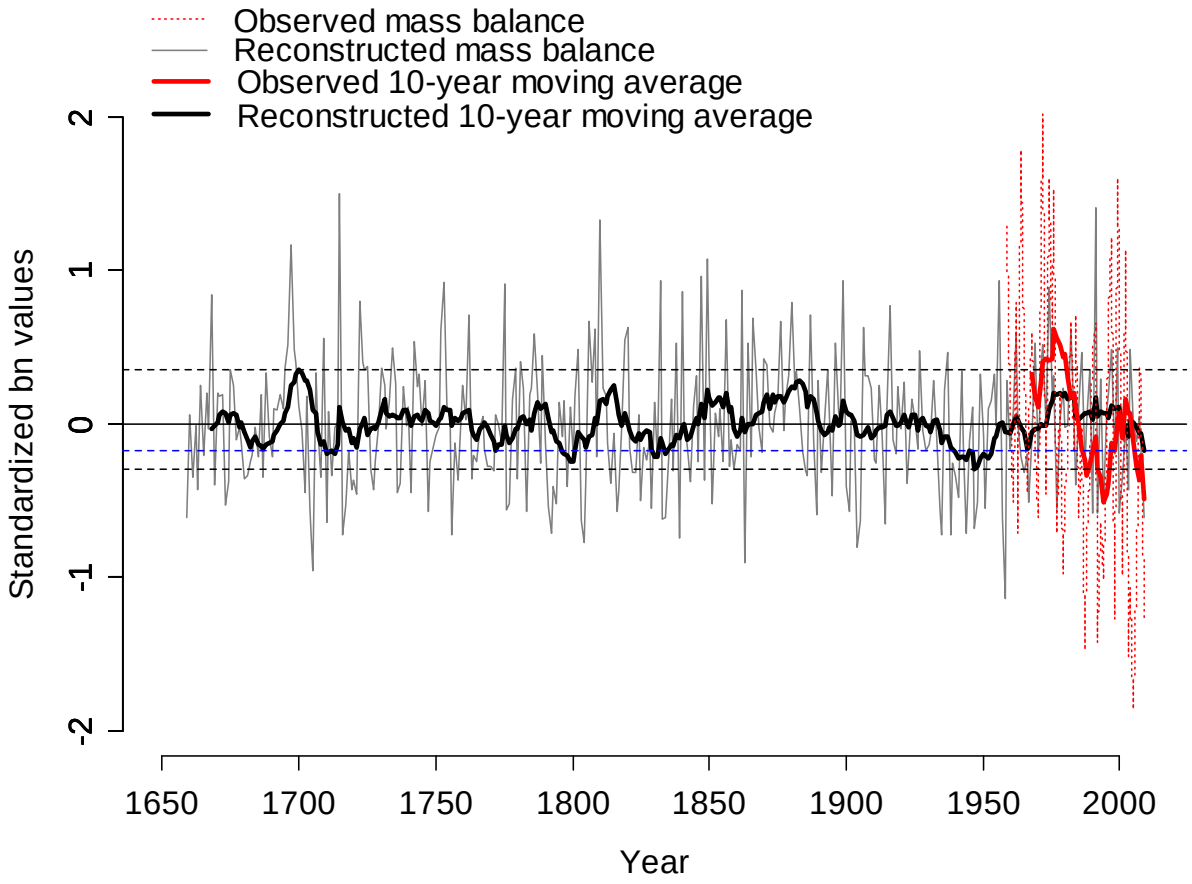

Figure 17: Time series plot of reconstructed net balance and observed net balance. The thick black line represents a 10-year moving average of the reconstructed balance, and the thick red line is a 10-year moving average for the observed net balance. The dashed lines represent the minimum and maximum values of the reconstructed moving average line. The blue dashed line represents the reconstructed moving average minimum for 2009.